Dynamics of Fluid-Conveying Pipes

Ali Fasihi

NARODOWE CENTRUM NAUKI

Lodz University of Technology
Department of Automation, Biomechanics and Mechatronics

university of groningen / faculty of science and engineering

Contents

Two basic aspects of the problem have been known for a long time

- Fire-hose instability
- Buckling instability

- Garden-hose instability
- Flutter instability

THE STUDY OF THE DYNAMICS OF PIPES

Has become well known because:

- On the same level as the classical problems
  (a column subjected to compressive loading and the rotating shaft)
- Capable of displaying a various interesting dynamical behavior

  (period-n, quasi-periodic, and chaotic motion)
- Belongs to a broader class of dynamical systems involving momentum transport:

  (such as high speed magnetic and paper tapes, band-saw blades, transmission chains and belts)

THE STUDY OF THE DYNAMICS OF PIPES

Travelling chains and elastic cords (A series of experiments by Aitken (1878))

Deriving the correct equations of motion Bourrières (1939)

The 1950s and 1960s (out of curiosity)

The applications came afterwards, 20, 30 and 50 years later

(For engineering applications, the phenomena of interest occured at flow velocities beyond the normal engineering range) (Escaping the interesting dynamics by increasing the cross-sectional flow area)

The advent of new applications (very long, thin-walled, or aspirating pipes)

has resulted in shifting the critical flow and bringing interesting dynamics into the normal operating range

(making them of direct interest to designers and operators, as well as researchers)

APPLICATIONS

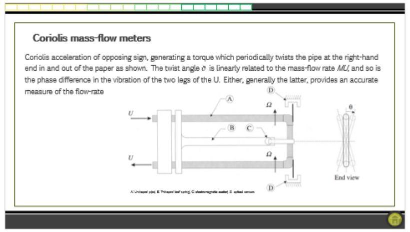

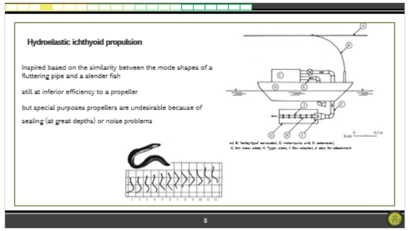

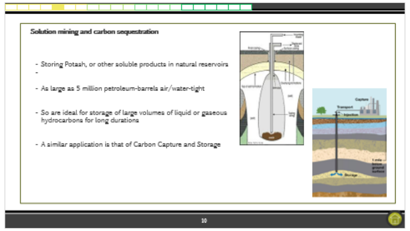

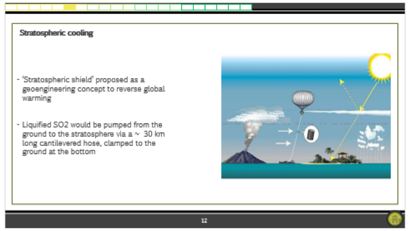

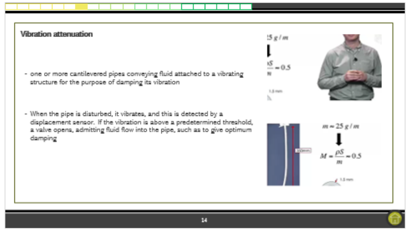

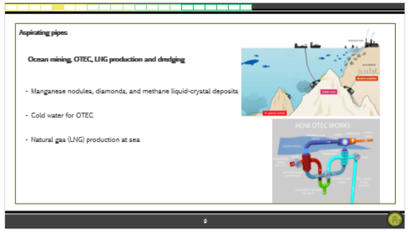

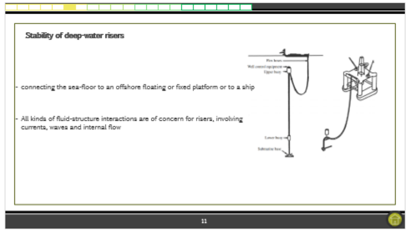

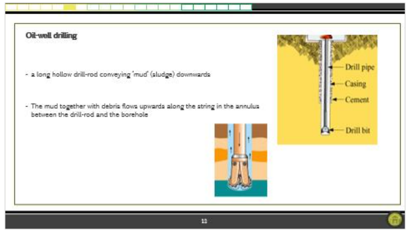

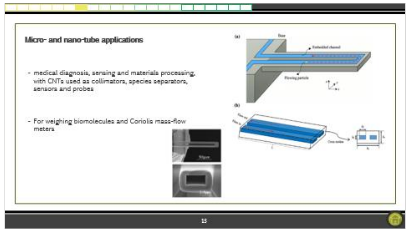

Coriolis mass-flow meters

Coriolis acceleration of opposing sign, generating a torque which periodically twists the pipe at the right-hand end in and out of the paper as shown. The twist angle ϑ is linearly related to the mass-flow rate *MU*, and so is the phase difference in the vibration of the two legs of the U. Either, generally the latter, provides an accurate measure of the flow-rate

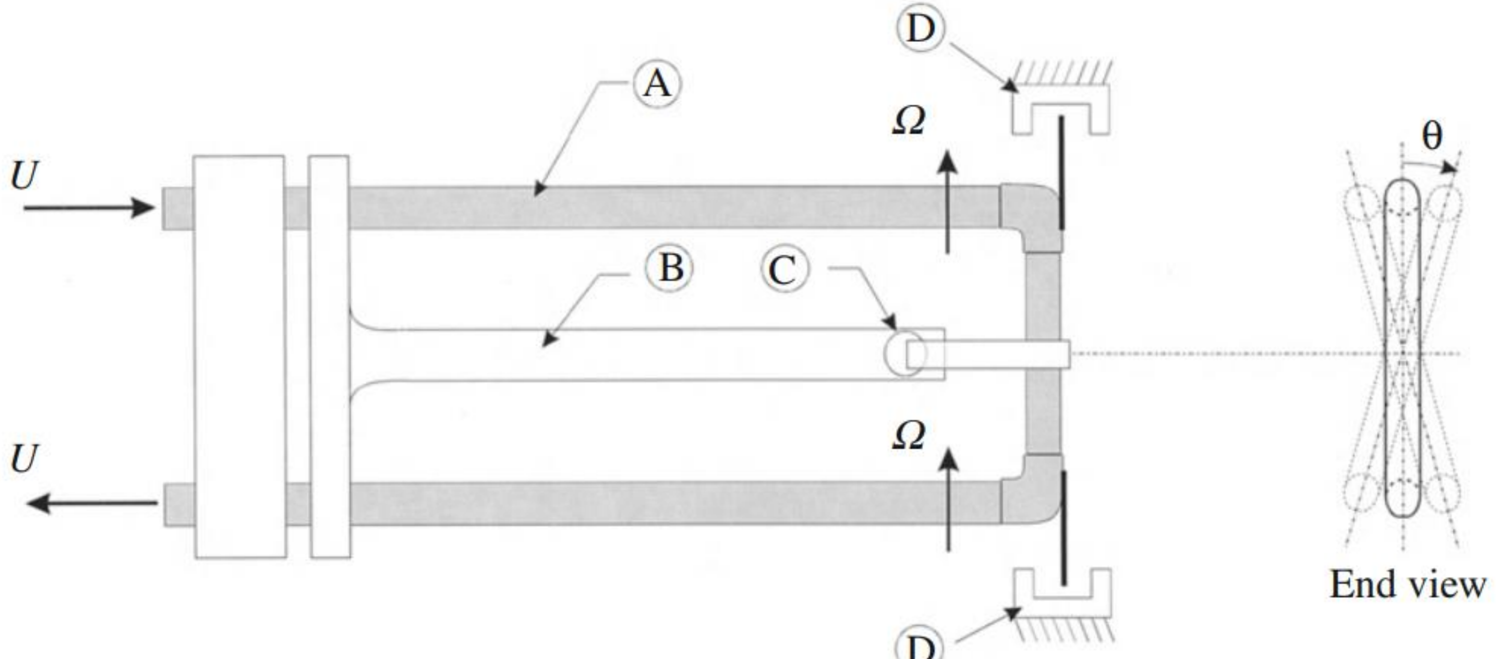

A: U-shaped pipe; B: T-shaped leaf spring; C: electromagnetic exciter; D: optical sensors

Hydroelastic ichthyoid propulsion

Inspired based on the similarity between the mode shapes of a fluttering pipe and a slender fish

still at inferior efficiency to a propeller

but special purposes propellers are undesirable because of

sealing (at great depths) or noise problems

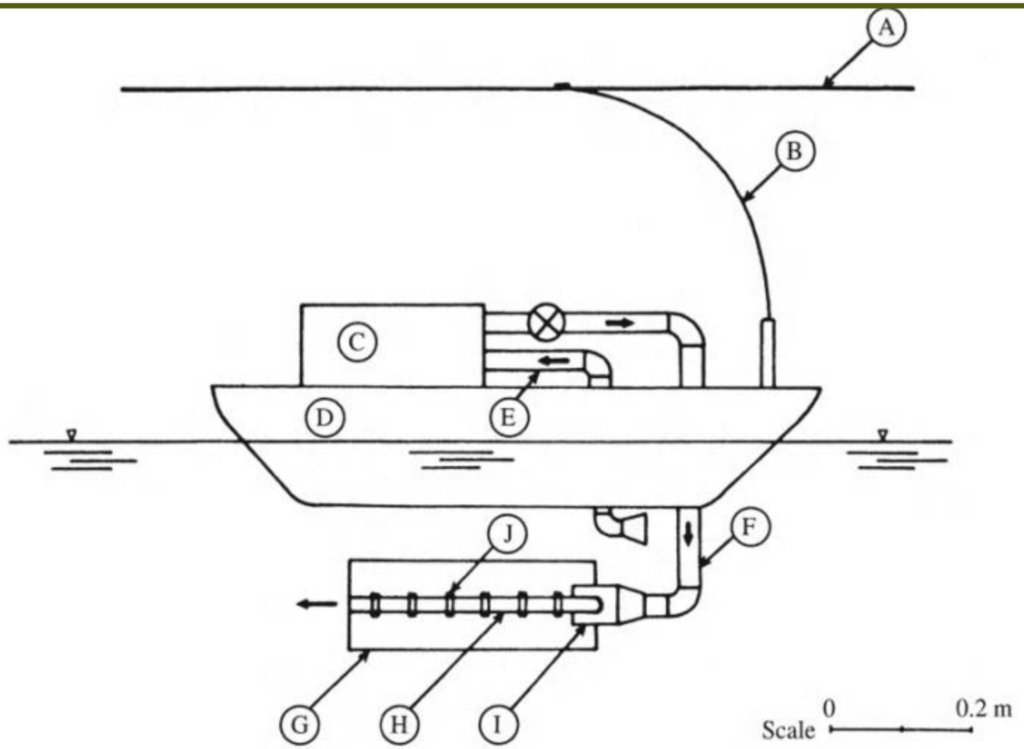

or; B: 'trolley-type' conductor; C: motor-pump unit; D: catamaran;
G: thin brass plate; H: Tygon pipes; I: flow adaptor; J: clips for attachment

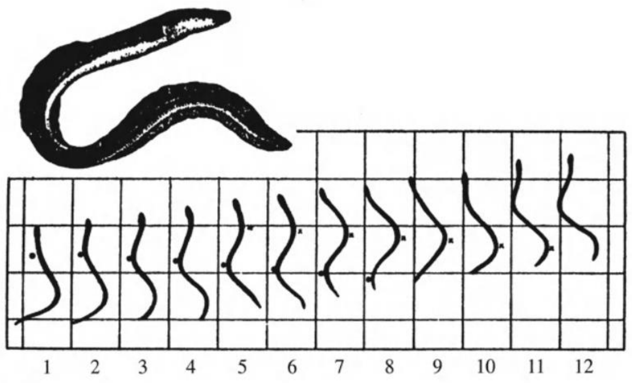

Aspirating pipes

Ocean mining, OTEC, LNG production and dredging

- Manganese nodules, diamonds, and methane liquid-crystal deposits
- Cold water for OTEC
- Natural gas (LNG) production at sea

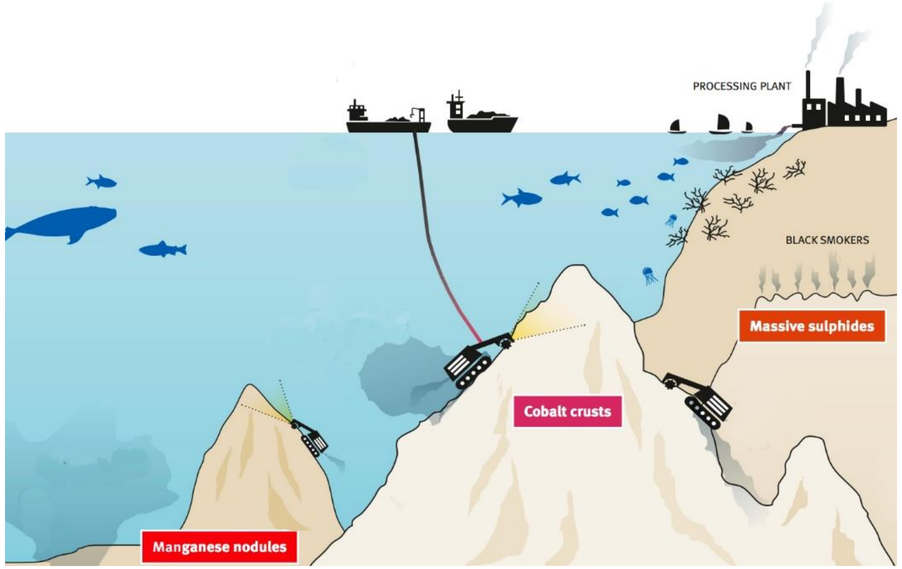

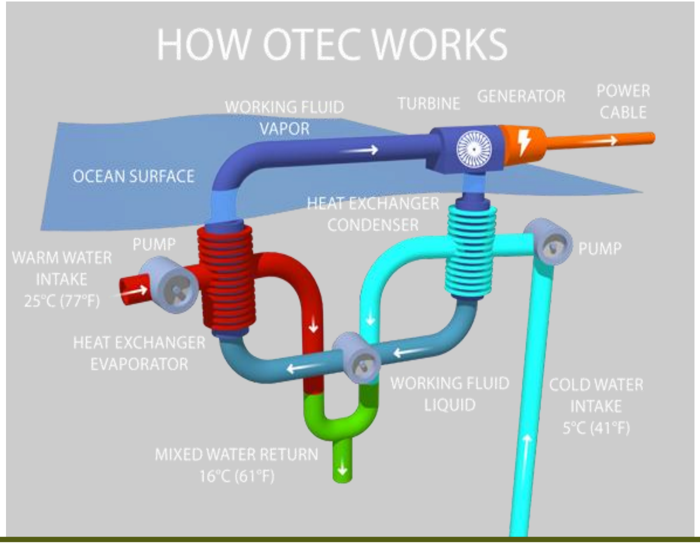

Solution mining and carbon sequestration

- Storing Potash, or other soluble products in natural reservoirs
-
- As large as 5 million petroleum-barrels air/water-tight
- So are ideal for storage of large volumes of liquid or gaseous hydrocarbons for long durations
- A similar application is that of Carbon Capture and Storage

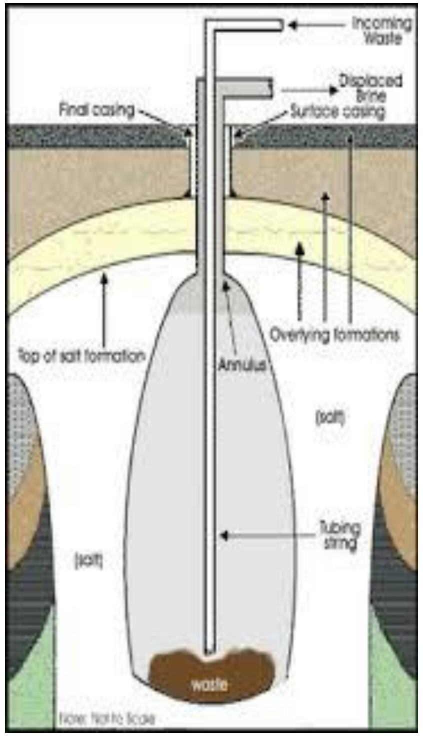

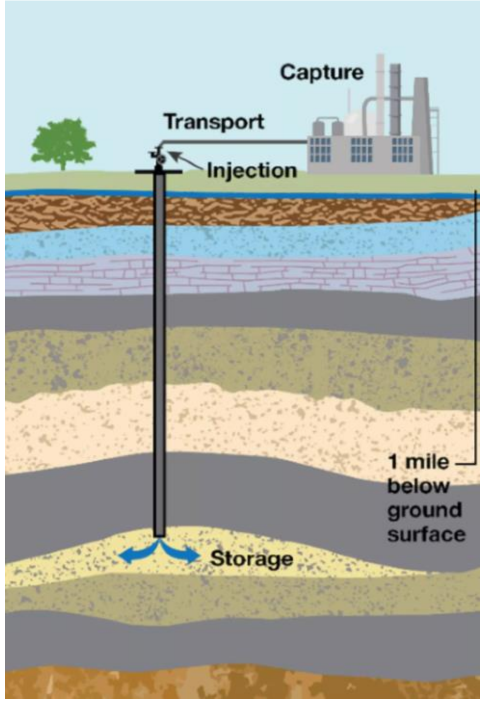

Stability of deep-water risers

- connecting the sea-floor to an offshore floating or fixed platform or to a ship

- All kinds of fluid-structure interactions are of concern for risers, involving currents, waves and internal flow

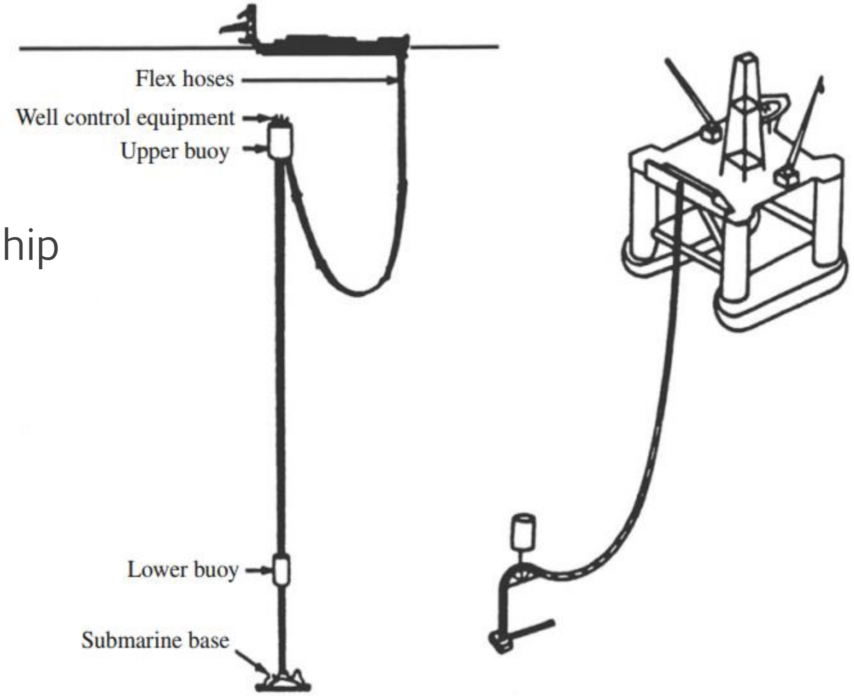

Stratospheric cooling

- ‘Stratospheric shield’ proposed as a geoengineering concept to reverse global warming

- Liquified SO_2 would be pumped from the ground to the stratosphere via a ~ 30 km long cantilevered hose, clamped to the ground at the bottom

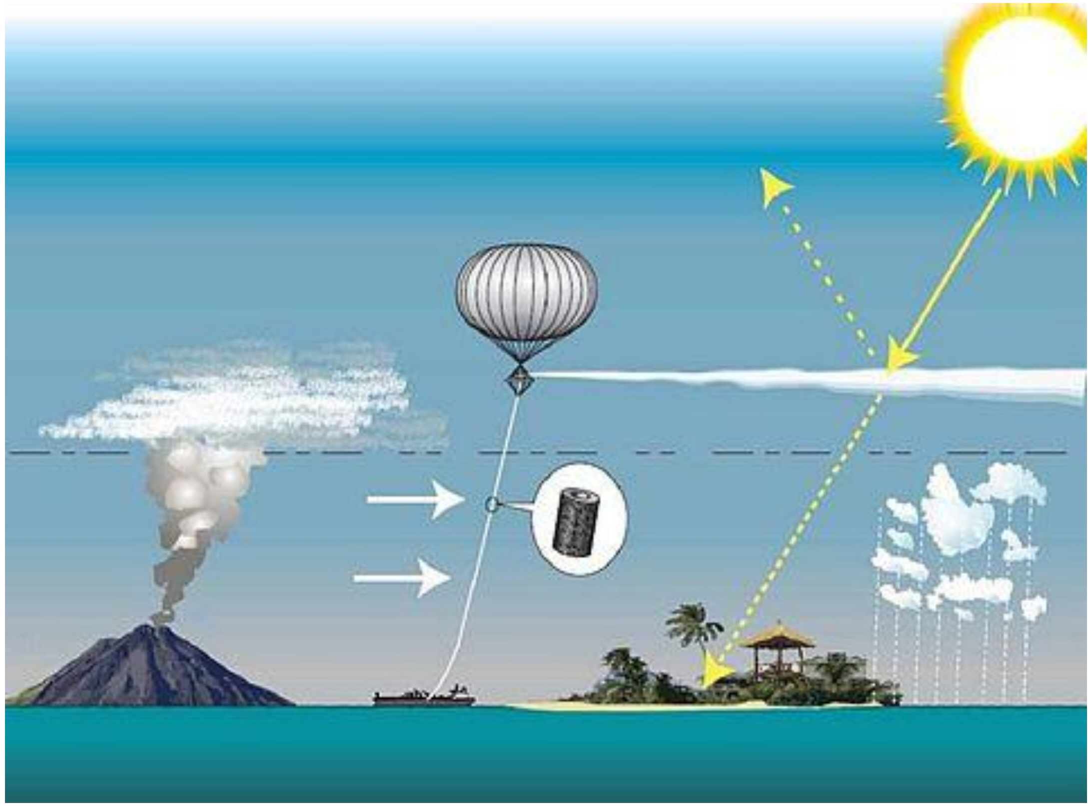

Oil-well drilling

- a long hollow drill-rod conveying 'mud' (sludge) downwards

- The mud together with debris flows upwards along the string in the annulus between the drill-rod and the borehole

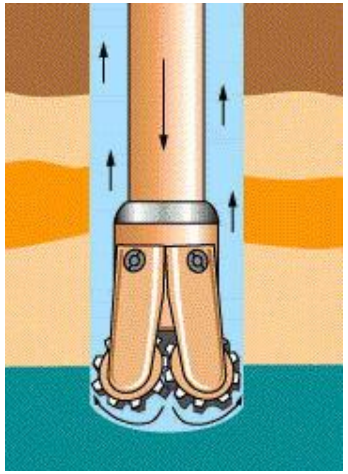

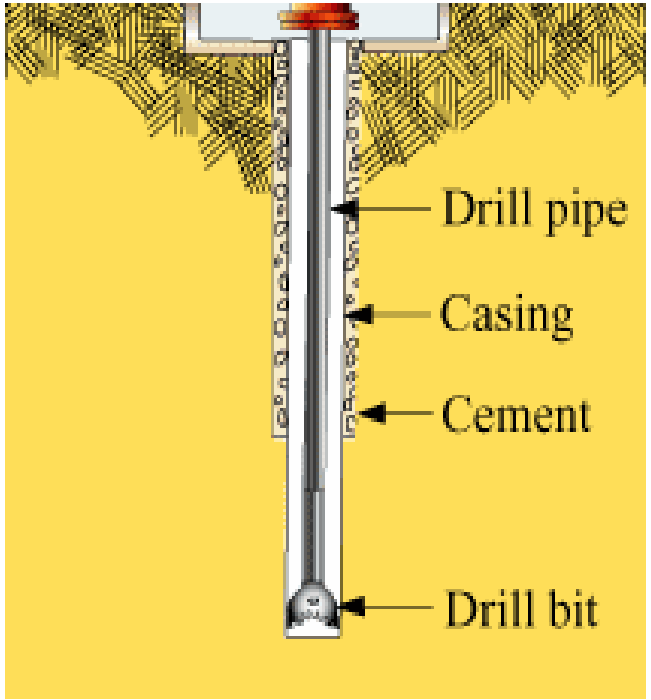

Vibration attenuation

- one or more cantilevered pipes conveying fluid attached to a vibrating structure for the purpose of damping its vibration

- When the pipe is disturbed, it vibrates, and this is detected by a displacement sensor. If the vibration is above a predetermined threshold, a valve opens, admitting fluid flow into the pipe, such as to give optimum damping

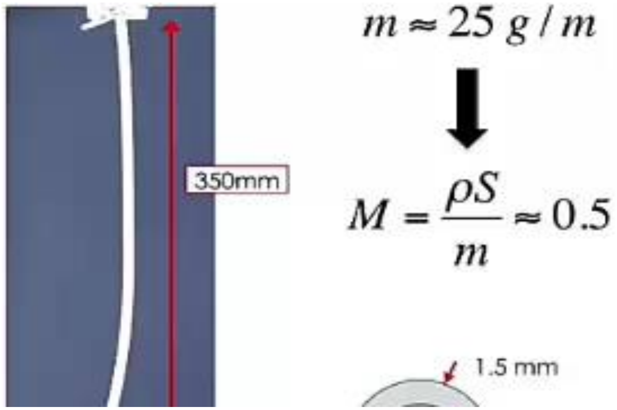

Micro- and nano-tube applications

- medical diagnosis, sensing and materials processing, with CNTs used as collimators, species separators, sensors and probes

- For weighing biomolecules and Coriolis mass-flow meters

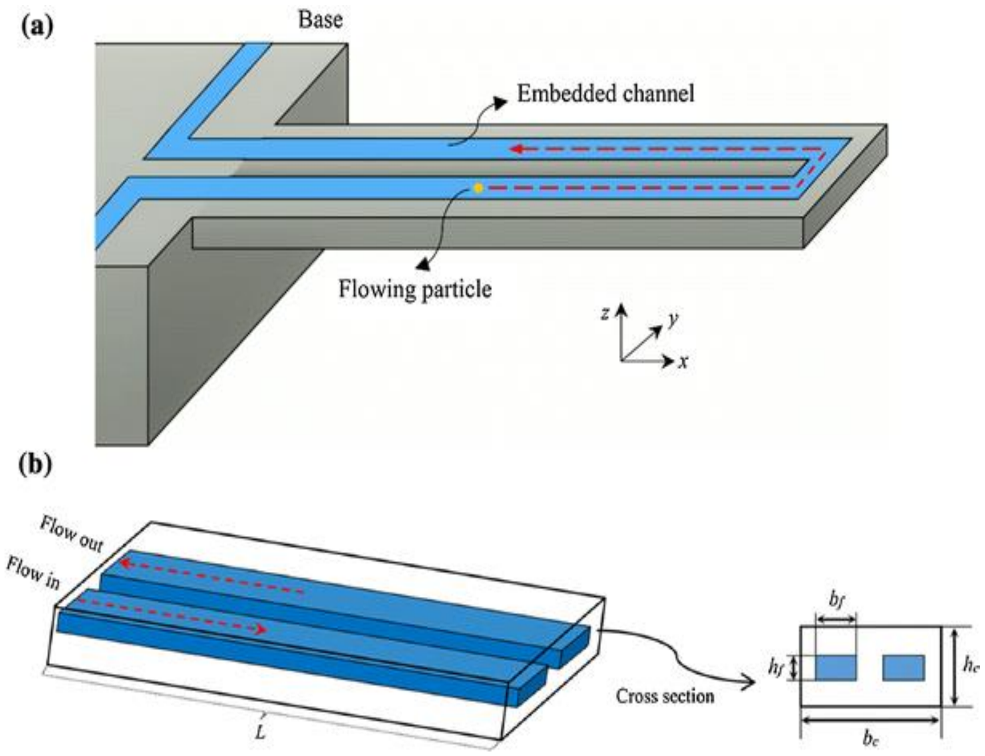

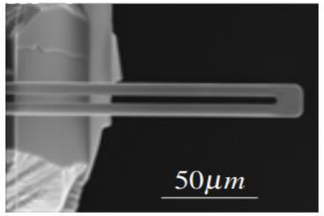

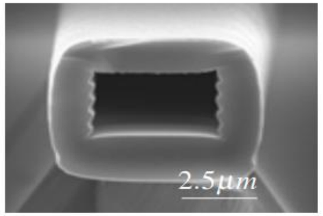

Problem at hand

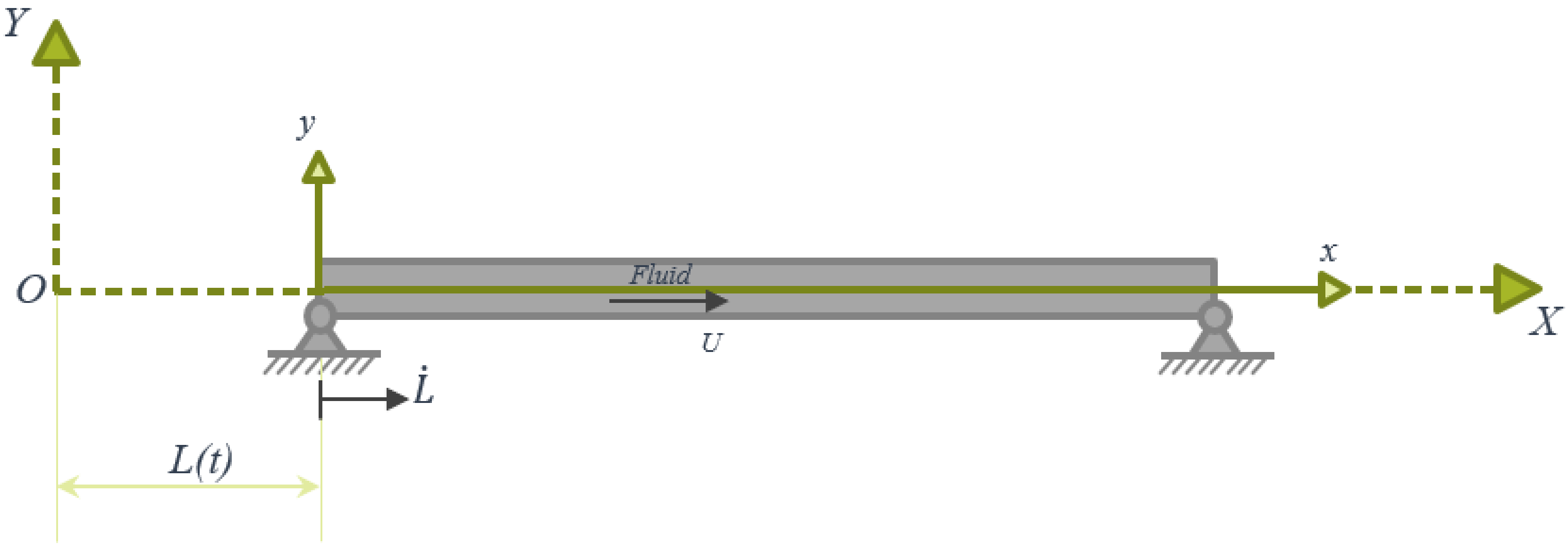

KINEMATICS

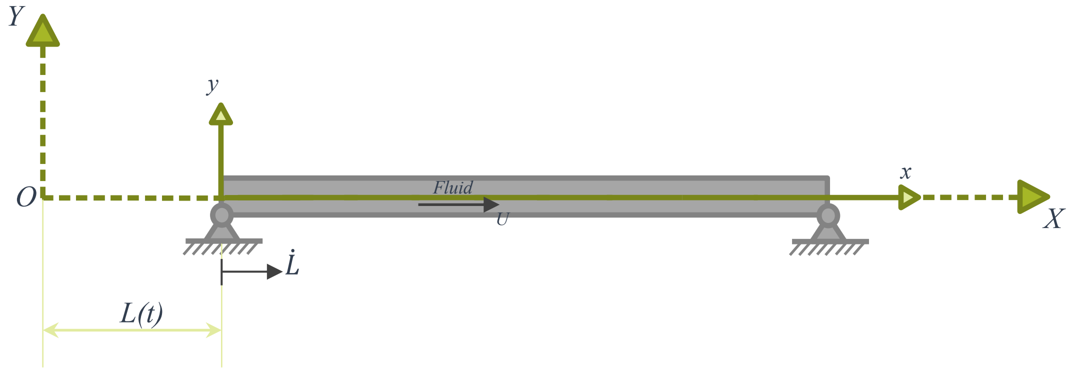

$$\vec{r}_{initial} = X_0\vec{i} + Y_0\vec{j} = (L(0) + x_0)\vec{i} + (y_0)\vec{j}$$

$$\vec{r} = X\vec{i} + Y\vec{j} = (L(t) + x)\vec{i} + (y)\vec{j}$$

$$u(X_0,t) = X - X_0 = X(X_0(t),t) - X_0(t)$$

$$w(Y_0,t) = Y - Y_0 = Y(Y_0(t),t) - Y_0(t)$$

The velocity and acceleration of the pipe

$$v_{pX} = \frac{DX}{Dt} = \frac{\partial u}{\partial t} + \frac{\partial u}{\partial X0}\frac{dX_0}{dt} = \frac{\partial u}{\partial t} + \dot{L}(t)\frac{\partial u}{\partial X_0}$$

$$v_{pY} = \frac{DY}{Dt} = \frac{\partial w}{\partial t} + \frac{\partial w}{\partial X_0}\frac{dX_0}{dt} = \frac{\partial w}{\partial t} + \dot{L}(t)\frac{\partial w}{\partial X_0}$$

$$a_{pX} = \frac{Dv_{pX}}{Dt} = \frac{\partial v_{pX}}{\partial t} + \dot{L}(t)\frac{\partial v_{pX}}{\partial X_0} \approx \left(\frac{\partial}{\partial t} + \dot{L}(t)\frac{\partial}{\partial X0}\right)^2 u$$

$$a_{pY} = \frac{Dv_{pY}}{Dt} = \frac{\partial v_{pY}}{\partial t} + \dot{L}(t)\frac{\partial v_{pY}}{\partial X_0} \approx \left(\frac{\partial}{\partial t} + \dot{L}(t)\frac{\partial}{\partial X_0}\right)^2 w$$

The velocity and acceleration of the internal fluid

$$v_{fX} = \left(\frac{\partial}{\partial t} + \dot{L}(t)\frac{\partial}{\partial X_0}\right)u + V\left(1 + \frac{\partial u}{\partial X_0}\right)$$

$$v_{fY} = \left(\frac{\partial}{\partial t} + \dot{L}(t)\frac{\partial}{\partial X_0}\right)w + V\frac{\partial w}{\partial X_0}$$

$$a_{fX} = \frac{Dv_{fX}}{Dt} = \frac{\partial v_{fX}}{\partial t} + \dot{L}(t)\frac{\partial v_{fX}}{\partial X0} \approx \left(\frac{\partial}{\partial t} + (\dot{L}(t)+V)\frac{\partial}{\partial X0}\right)^2 u + \dot{V}$$

$$a_{fY} = \frac{Dv_{fY}}{Dt} = \frac{\partial v_{fY}}{\partial t} + \dot{L}(t)\frac{\partial v_{fY}}{\partial X0} \approx \left(\frac{\partial}{\partial t} + (\dot{L}(t)+V)\frac{\partial}{\partial X0}\right)^2 w$$

FORCES

The free-body diagram of an element of the pipe

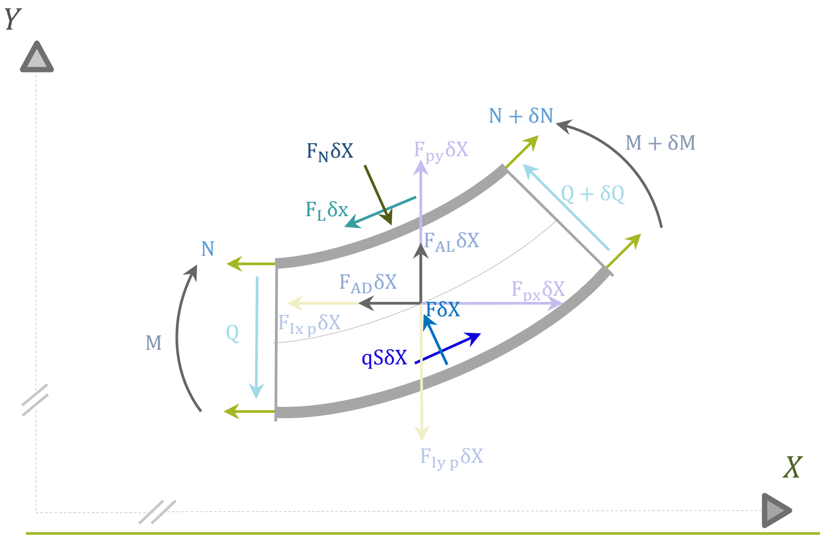

N	longitudinal tension
Q	Shear force
M	the bending moment
F	the internal fluid and the pipe interaction force
qS	the internal fluid and the pipe interaction force
F_{px} , F_{py}	hydrostatic forces
F_{AD} , F_{AL}	additional inertia forces
F_N , F_L	viscous forces
F_{Ix} , F_{Iy}	inertia forces

The free-body diagram of an element of the internal fluid

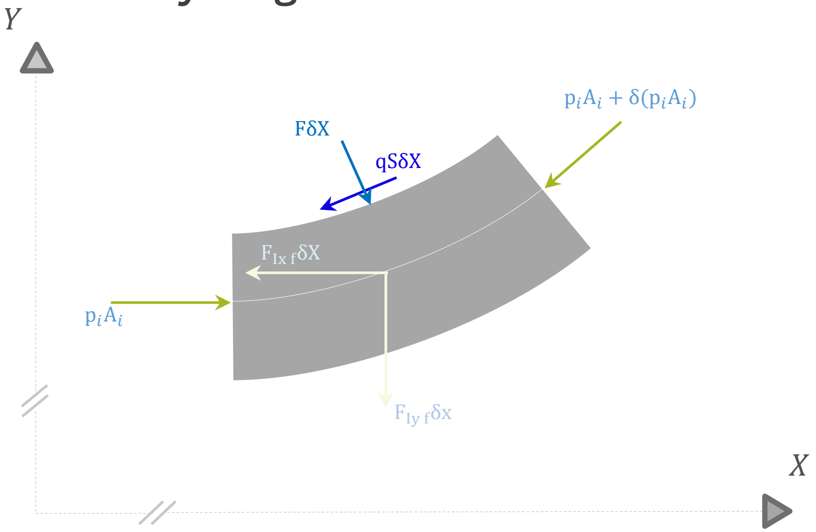

p_i A_i	hydrostatic pressure
F	the internal fluid and the pipe interaction force
qS	the internal fluid and the pipe interaction force
F_{Ix} , F_{Iy}	inertia forces

EQUATIONS OF MOTION

The equations of the axial and lateral motions

$$-\frac{\partial N}{\partial X}+\frac{\partial}{\partial X}(p_i A_i)+m_f\left(\left(\frac{\partial}{\partial t}+(\dot{L}+V)\frac{\partial}{\partial X}\right)^2 u+\dot{V}\right)$$
$$+(\beta M+m_p)\left(\frac{\partial}{\partial t}+\dot{L}\frac{\partial}{\partial X}\right)^2 u+\frac{1}{2}C_T\left(\frac{M}{D}\right)\dot{L}^2-\frac{\partial}{\partial X}(p_o A_o)+\frac{\partial p_o}{\partial X}(A_o)=0$$

$$-\frac{\partial}{\partial X}\left(N\frac{\partial w}{\partial X}\right)+EI\frac{\partial}{\partial X}\left(\frac{\partial^3 w}{\partial X^3}\right)+\frac{\partial}{\partial X}\left(p_i A_i\frac{\partial w}{\partial X}\right)+m_f\left(\frac{\partial}{\partial t}+(\dot{L}+V)\frac{\partial}{\partial X}\right)^2 w$$
$$+M\left(\frac{\partial}{\partial t}+\beta\dot{L}\frac{\partial}{\partial X}\right)^2 w+\frac{1}{2}\dot{L}C_N\left(\frac{M}{D}\right)\left(\frac{\partial w}{\partial t}+\dot{L}\frac{\partial w}{\partial X}\right)$$
$$+\frac{1}{2}\widetilde{C_N}\left(\frac{M}{D}\right)\left(\frac{\partial w}{\partial t}+\dot{L}\frac{\partial w}{\partial X}\right)+\frac{1}{2}C_T\left(\frac{M}{D}\right)\dot{L}^2\frac{\partial w}{\partial X}-\frac{\partial}{\partial X}(p_o A_o)\frac{\partial w}{\partial X}$$
$$+m_p\left(\frac{\partial}{\partial t}+\dot{L}\frac{\partial}{\partial X}\right)^2 w=0$$

Stretching effect

$$N_{nonlinear}=\frac{EA}{2l}\int_0^l\left(\frac{\partial w}{\partial x}\right)^2 dx$$

$$EIw''''+\left[m_f V^2+M\left((\beta-1)\dot{L}(t)\right)^2\right.$$
$$+\left(m_f\dot{V}+(m_f+\beta M+m_p)\ddot{L}(t)+\frac{1}{2}C_T\left(\frac{M}{D}\right)\dot{L}(t)^2+\frac{\partial p_o}{\partial x}(A_o)\right)(l$$
$$\left.-x)+\frac{EA}{2l}\int_0^l w'^2\,dX\right]w''-\left(\frac{\partial p_o}{\partial x}(A_o)+(m_f+\beta M+m_p)\ddot{L}(t)\right)w'$$
$$+2\left(m_f V+M(\beta-1)\dot{L}(t)\right)\dot{w}'+\frac{1}{2}\dot{L}(C_N+\widetilde{C_N})\left(\frac{M}{D}\right)\dot{w}$$
$$+(m_p+m_f+M)\ddot{w}=0$$

MAKING DIMENSIONLESS AND DISCRETIZATION

Discretization

$$\eta = \frac{w}{l}, \qquad \xi = \frac{x}{l}, \qquad \tau = \left(\frac{EI}{m_f + \beta M + m_p}\right)^2 \frac{t}{l^2} = \sigma t$$

$$u = \left(\frac{m_f}{EI}\right)^{1/2} lV, \qquad v = \left(\frac{M}{EI}\right)^{1/2} l\dot{L}(t)$$

$$\beta_1 = \frac{m_f}{m_f + \beta M + m_p}, \beta_2 = \frac{m_p}{m_f + \beta M + m_p}, \beta_3 = \frac{M}{m_f + \beta M + m_p} = 1 - \beta_1 - \beta_2$$

$$\varepsilon = \frac{l}{D}, \quad \bar{c} = \frac{\widetilde{C_N}}{\sigma l}, \quad \boldsymbol{\mu} = \frac{l^2 A}{I} = 16\left(\frac{l}{D}\right)^2 = 16\varepsilon^2, \qquad int = \int_0^1 \left(\frac{\partial \eta}{\partial \xi}\right)^2 d\xi$$

$$\eta'''' + \left[u^2 + (\beta - 1)^2 v + \left(\beta_1{}^{1/2}\dot{u} + (1 - \beta_3 + \beta\beta_3)\beta_3{}^{-1/2}\dot{v} + \frac{1}{2}C_T \varepsilon v^2\right)(1 - \xi) + \frac{1}{2}\mu\, int\right]\eta'' - \beta_3{}^{-1/2}\dot{v}\eta' + 2\left(\beta_1{}^{1/2}u + (\beta - 1)\,\beta_3{}^{1/2}v\right)\dot{\eta}' + \frac{1}{2}\varepsilon\left(vC_N\beta_3{}^{1/2} + \beta_3\widetilde{C_N}\right)\dot{\eta} + \ddot{\eta} = 0$$

Making dimensionless

$$\eta(\xi, \tau) = \sum_{j=1}^{n} \varphi_j(\xi)\, q_j(\tau)$$

$$\boldsymbol{M\ddot{q}} + \boldsymbol{C\dot{q}} + \boldsymbol{Kq} + \boldsymbol{N(q)} = 0$$

$$M_{ij} = \int_0^1 \varphi_j(\xi)\varphi_i(\xi)\, d\xi$$

$$C_{ij} = 2\left(\beta_1^{\frac{1}{2}}u + (\beta - 1)\,\beta_3^{\frac{1}{2}}v\right)\int_0^1 \varphi_j{}'(\xi)\varphi_i(\xi)\, d\xi + \frac{1}{2}\varepsilon\left(vC_N\beta_3^{\frac{1}{2}} + \beta_3\widetilde{C_N}\right)\int_0^1 \varphi_j(\xi)\varphi_i(\xi)\, d\xi$$

$$K_{ij} = \int_0^1 \varphi_j{}''''(\xi)\varphi_i(\xi)\, d\xi + \left(u^2 + (\beta - 1)^2 v + \left(\beta_1{}^{1/2}\dot{u} + (1 - \beta_3 + \beta\beta_3)\beta_3{}^{-1/2}\dot{v} + \frac{1}{2}C_T\varepsilon v^2\right)\right)\int_0^1 \varphi_j{}''(\xi)\varphi_i(\xi)\, d\xi - \left(\beta_1^{\frac{1}{2}}\dot{u} + (1 - \beta_3 + \beta\beta_3)\beta_3^{-\frac{1}{2}}\dot{v} + \frac{1}{2}C_T\varepsilon v^2\right)\int_0^1 \xi\varphi_j{}''(\xi)\varphi_i(\xi)\, d\xi - \beta_3{}^{-1/2}\dot{v}\int_0^1 \varphi_j{}'(\xi)\varphi_i(\xi)\, d\xi$$

LINEAR ANALYSIS

$$M\ddot{\boldsymbol{q}} + C\dot{\boldsymbol{q}} + K\boldsymbol{q} = 0$$

$$\boldsymbol{q} = \boldsymbol{p}e^{i\omega\tau}$$

$$\left(-\omega^2\boldsymbol{M} + i\omega\,\mathbf{C} + \mathbf{K}\right)\boldsymbol{p} = 0$$

U=0.01

	Bifurcation	Divergence	Flutter
1st Frequency	3.532	3.533	7.28
2nd Frequency	-	-	-
3rd Frequency	10.61	10.62	-
4th Frequency	-	-	-

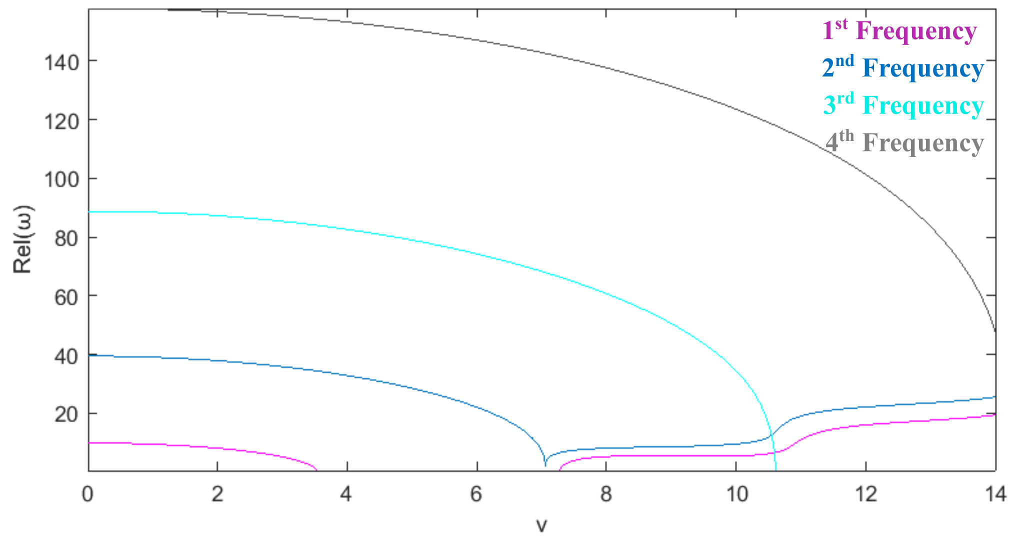

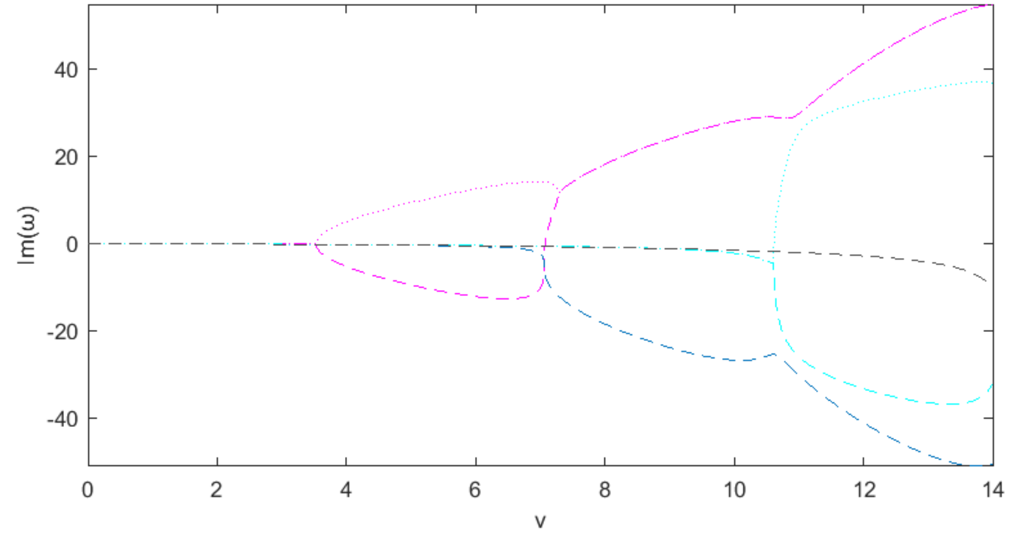

U=0.5

	Bifurcation	Divergence	Flutter
1st Frequency	3.487	3.488	7.32
2nd Frequency	7.43	7.55 - 7.58	-
3rd Frequency	10.59	10.6	-
4th Frequency	-	-	-

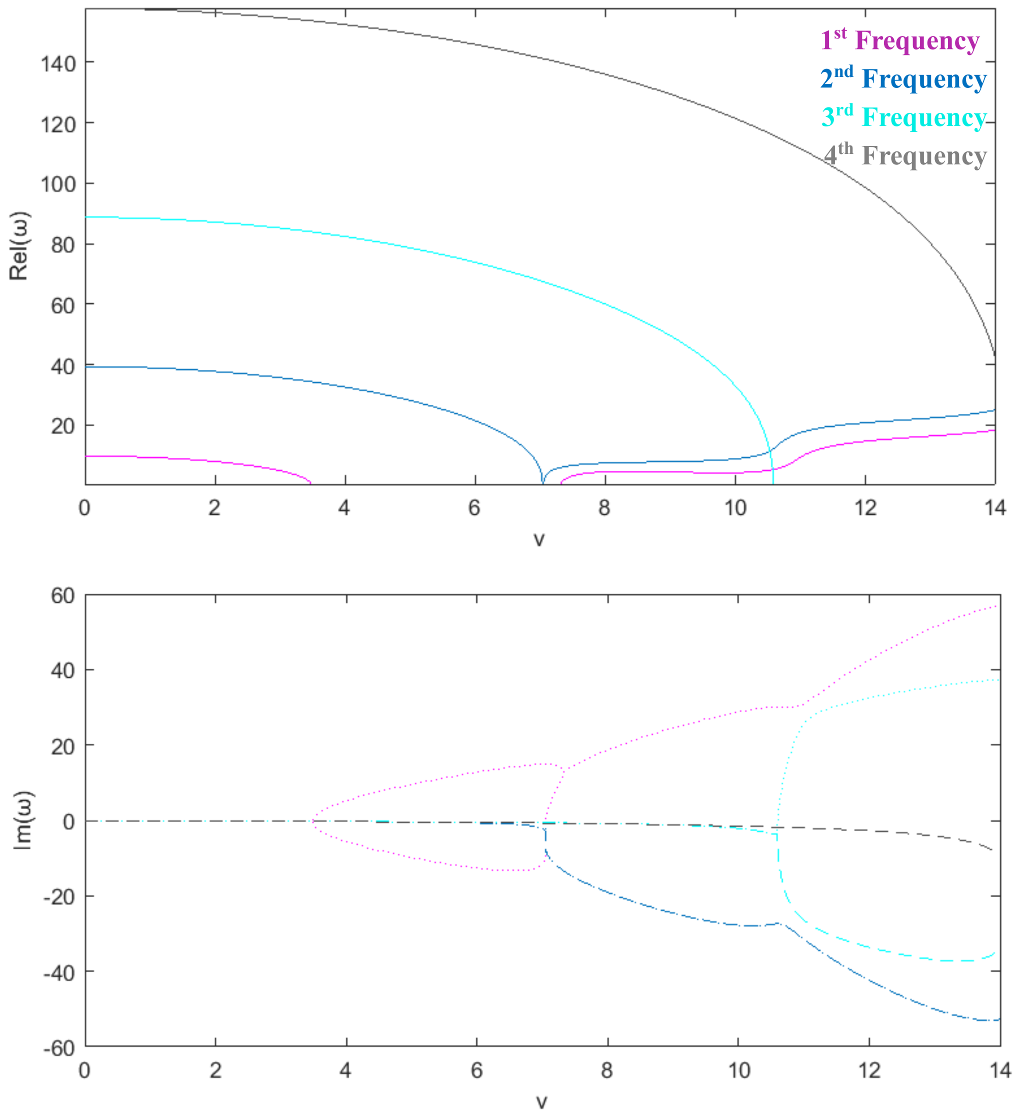

U=1.5

	Bifurcatio n	Divergence	Flutter	2nd Divergence	2nd Flutter
1st Frequency	3.1	3.105	7.33	9.13	10.7
2nd Frequency	6.84	6.86 - 6.98	-	-	-
3rd Frequency	10.48	10.49	-	-	-
4th Frequency	-	-	-	-	-

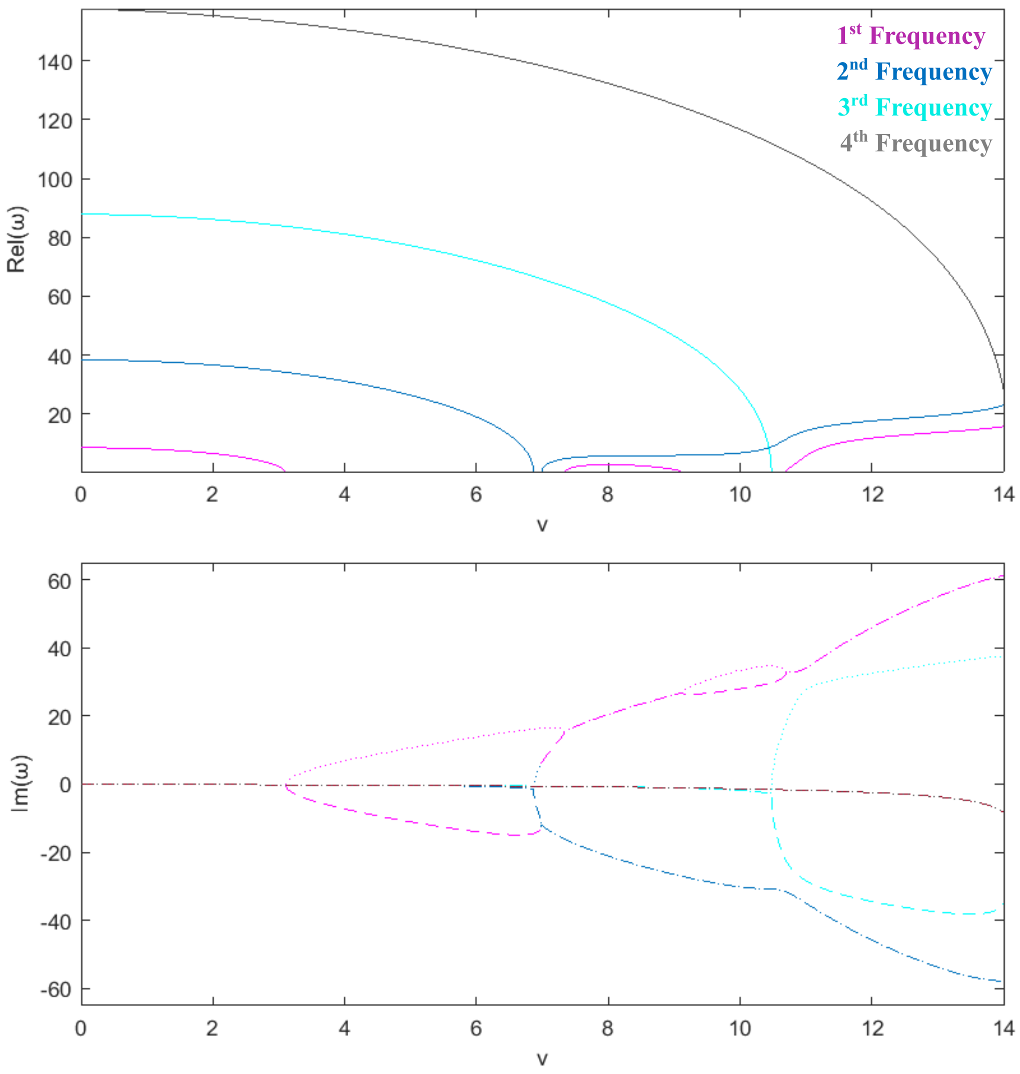

U=2.5

	Bifurcation	Divergence	Flutter
1st Frequency	2.14	3.105	10.92
2nd Frequency	6.47	6.48 - 6.84	-
3rd Frequency	10.22	10.23	-
4th Frequency	13.93	13.94	-

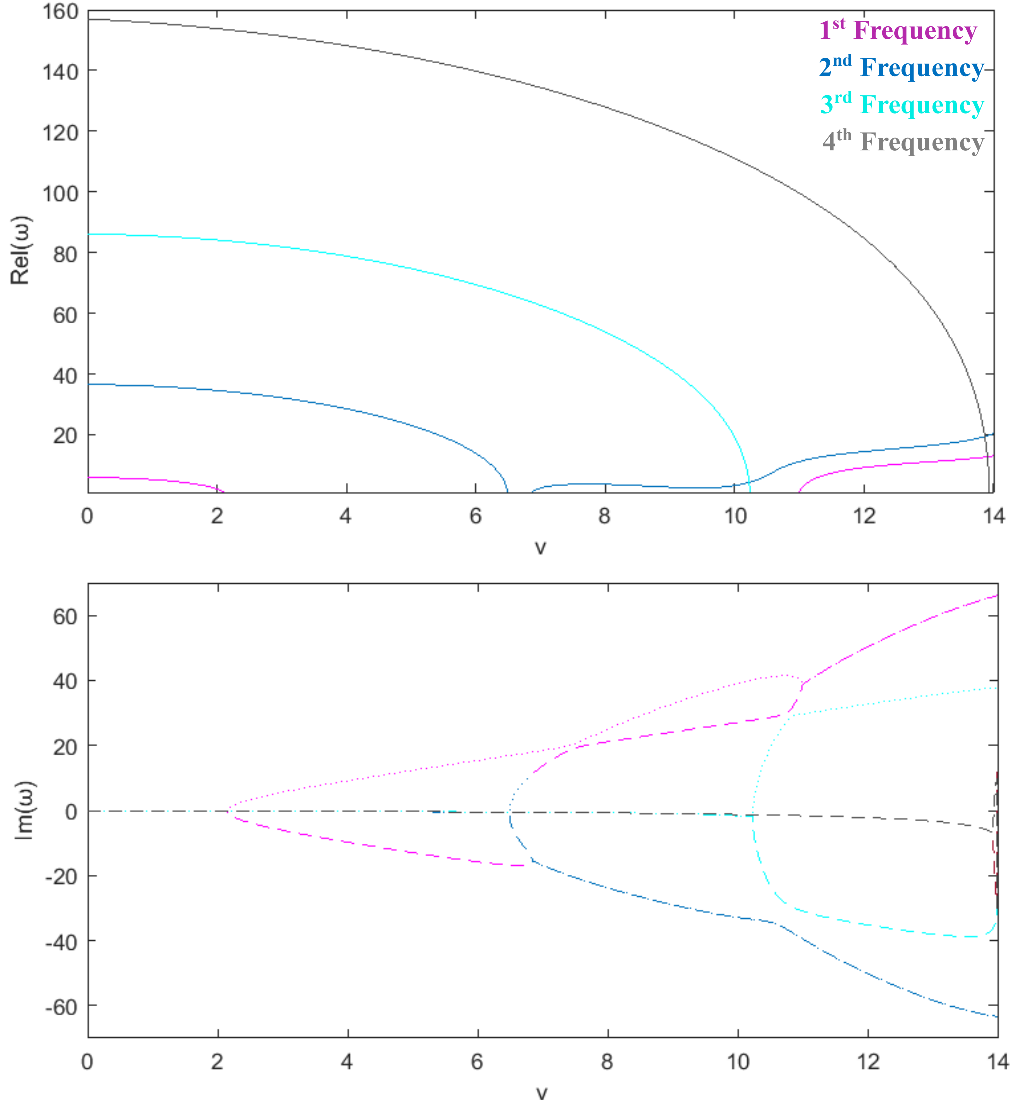

U=2.5

	Bifurcation	Divergence	Flutter
1st Frequency	2.14	3.105	10.92
2nd Frequency	6.47	6.48 - 6.84	-
3rd Frequency	10.22	10.23	-
4th Frequency	13.93	13.94	-

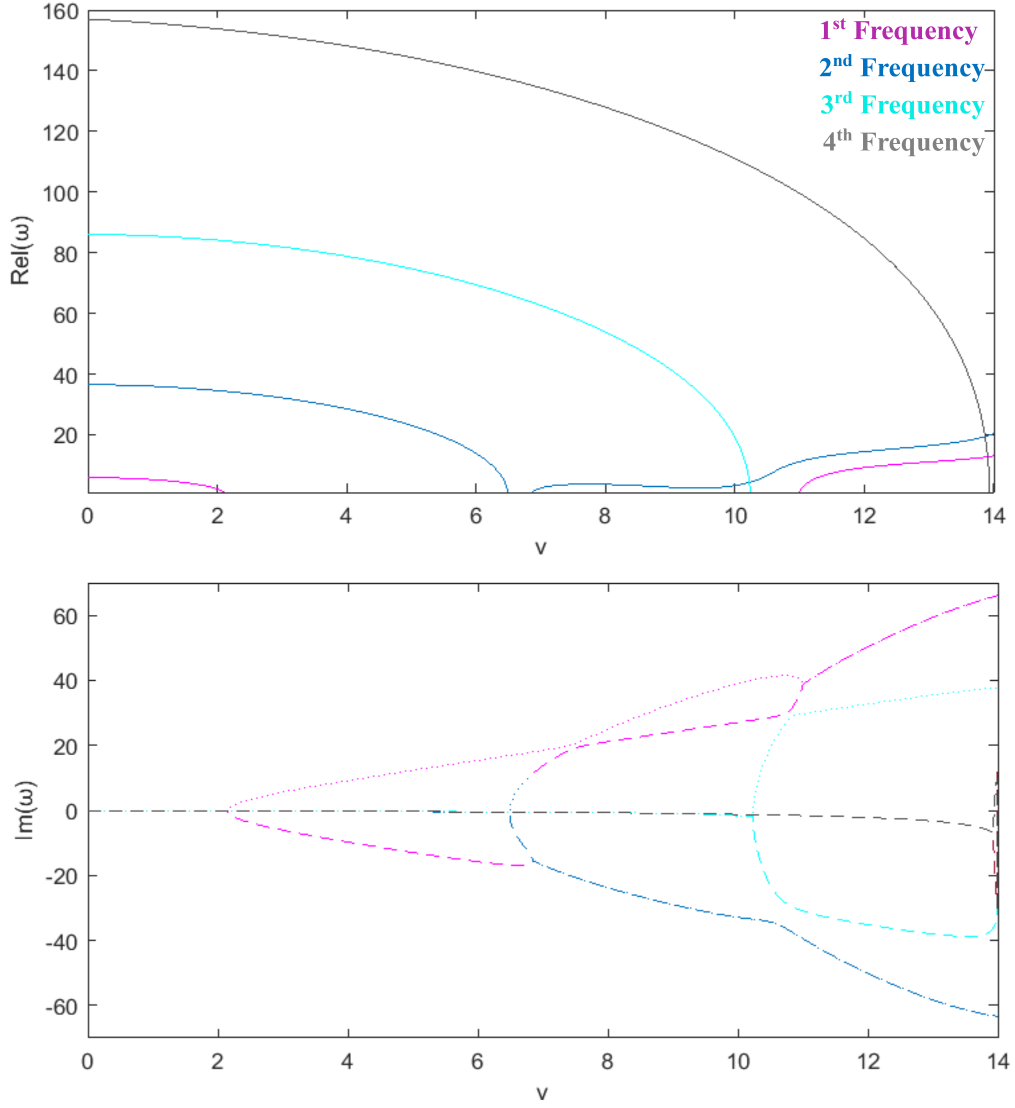

U=2.5

	Bifurcation	Divergence	Flutter
1st Frequency	2.14	3.105	10.92
2nd Frequency	6.47	6.48 - 6.84	-
3rd Frequency	10.22	10.23	-
4th Frequency	13.93	13.94	-

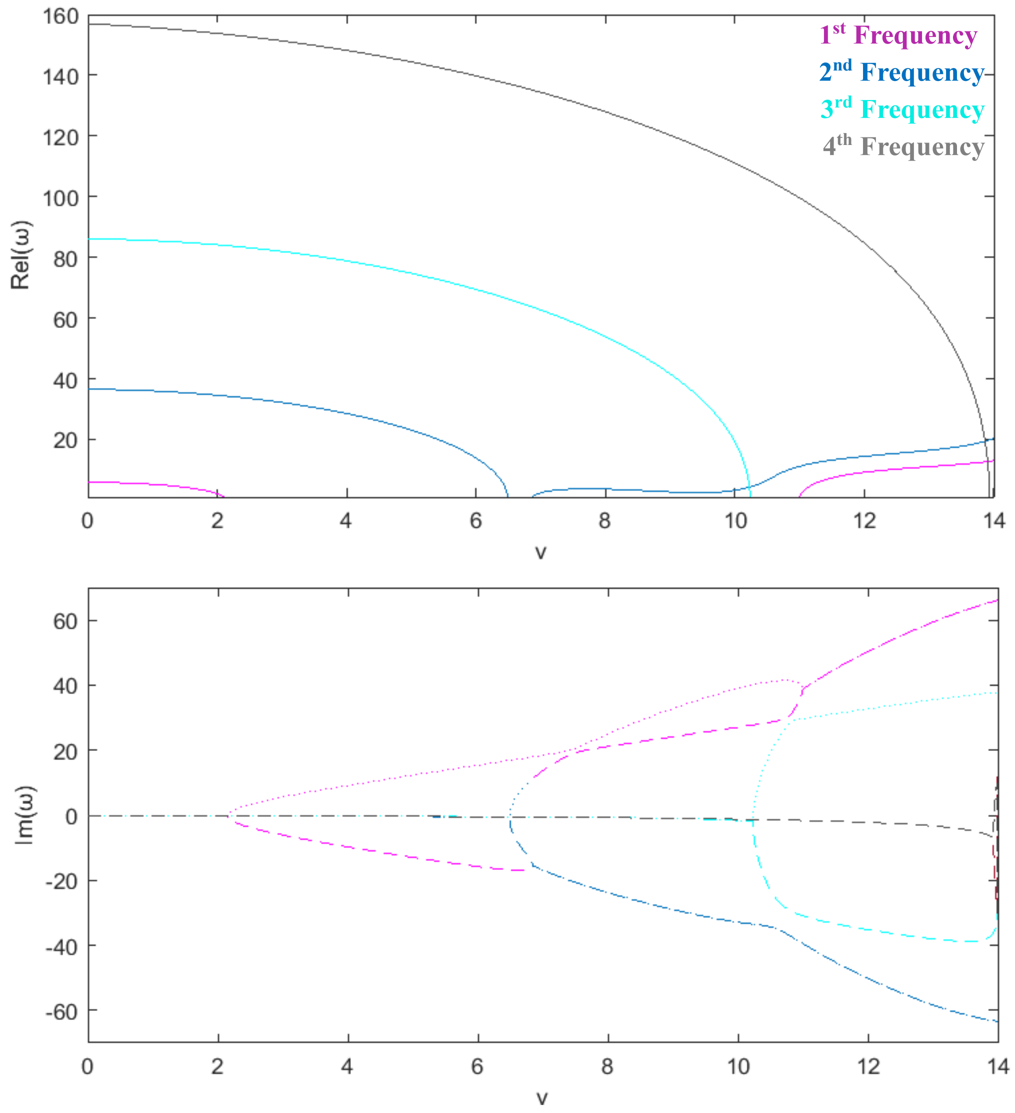

General Trends:

The frequency analysis reveals consistent patterns as internal flow velocity increases from u = 0.01 to u = 2.5:

- Bifurcation speed reduction: All modes exhibit decreased bifurcation speeds, with the first mode showing the most significant reduction of 1.39 (from 3.53 to 2.14), while higher modes show smaller reductions of 0.55 and 0.41 for the second and third modes,
- Flutter speed increase:
- The first mode flutter speed increases dramatically from vf1 = 7.28 to vf1 = 10.99, representing a 51% increase and demonstrating that internal flow delays flutter onset.
- Mode-dependent sensitivity: Lower modes exhibit greater sensitivity to internal flow variations, with the first mode experiencing the largest absolute changes in both bifurcation and flutter speeds.
- Stability margin enhancement: The increasing gap between bifurcation and flutter speeds at higher u values indicates enhanced post-buckling stability regions.

In the next section, these stability thresholds are obtained using the nonlinear model to provide more accurate predictions of the system’s post-critical behavior.

NONLINEAR STABILITY ANALYSIS

To evaluated the results obtained from frequency analysis, a nonlinear stability analysis was conducted using the pseudo-arclength continuation method

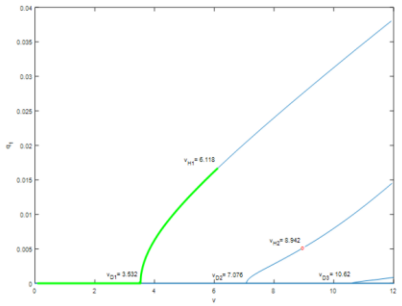

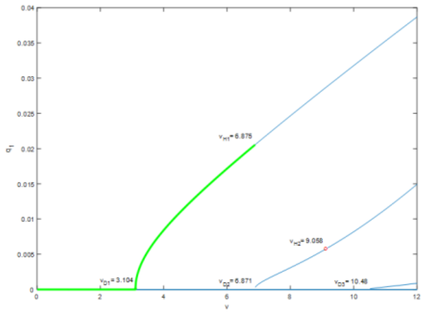

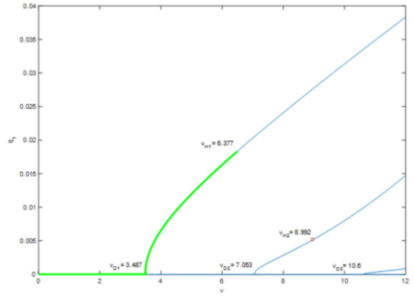

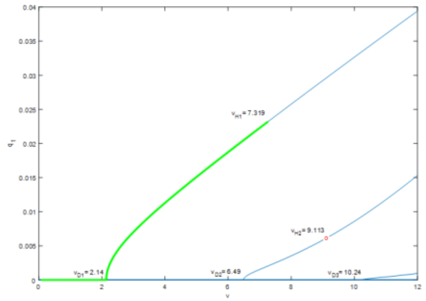

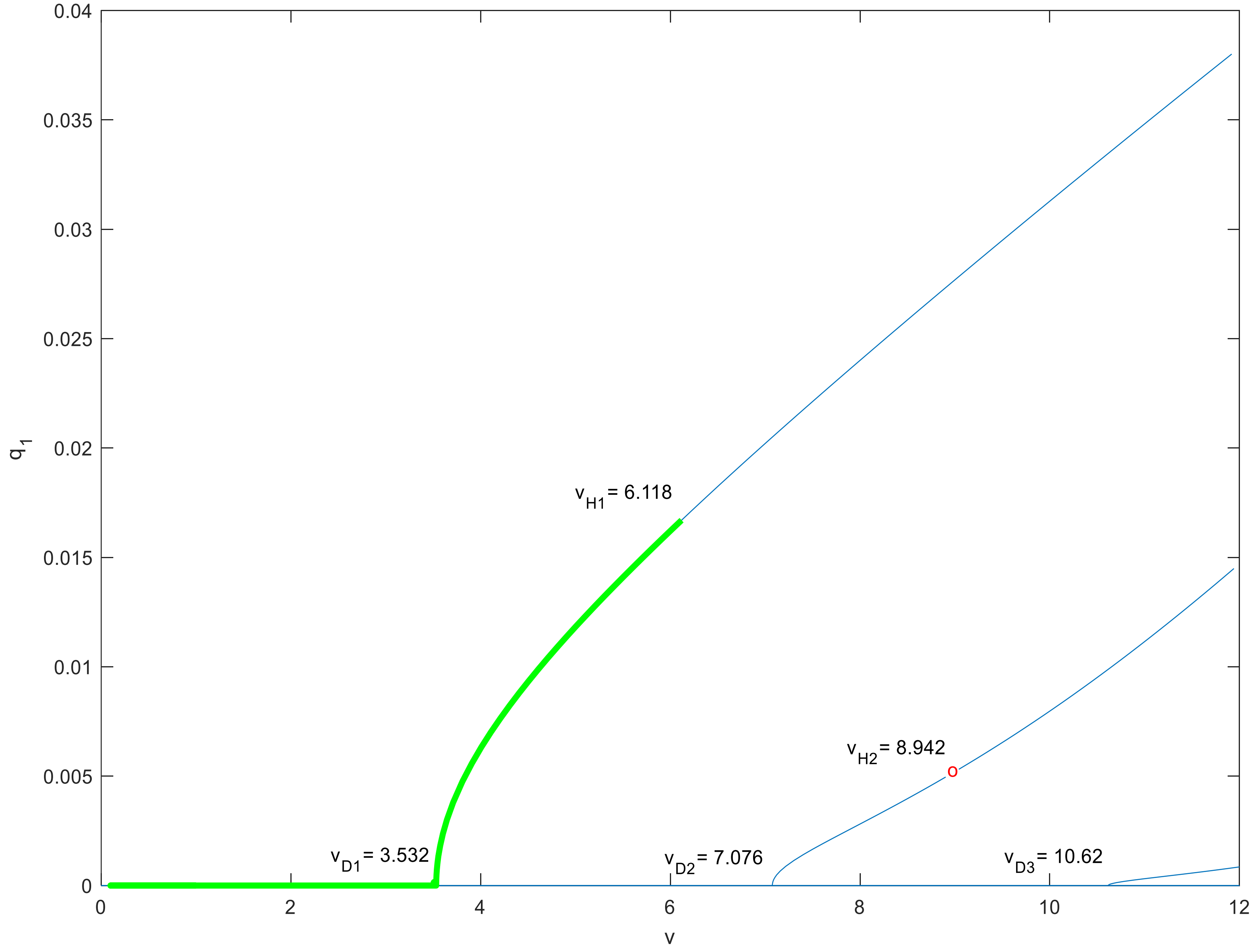

0.04
0.035
0.03
0.025
0.02
0.015
0.01
0.005
0
q1
0
2
4
6
8
10
12
v
vH1 = 6.118
vH2 = 8.942
vD1 = 3.532
vD2 = 7.076
vD3 = 10.62

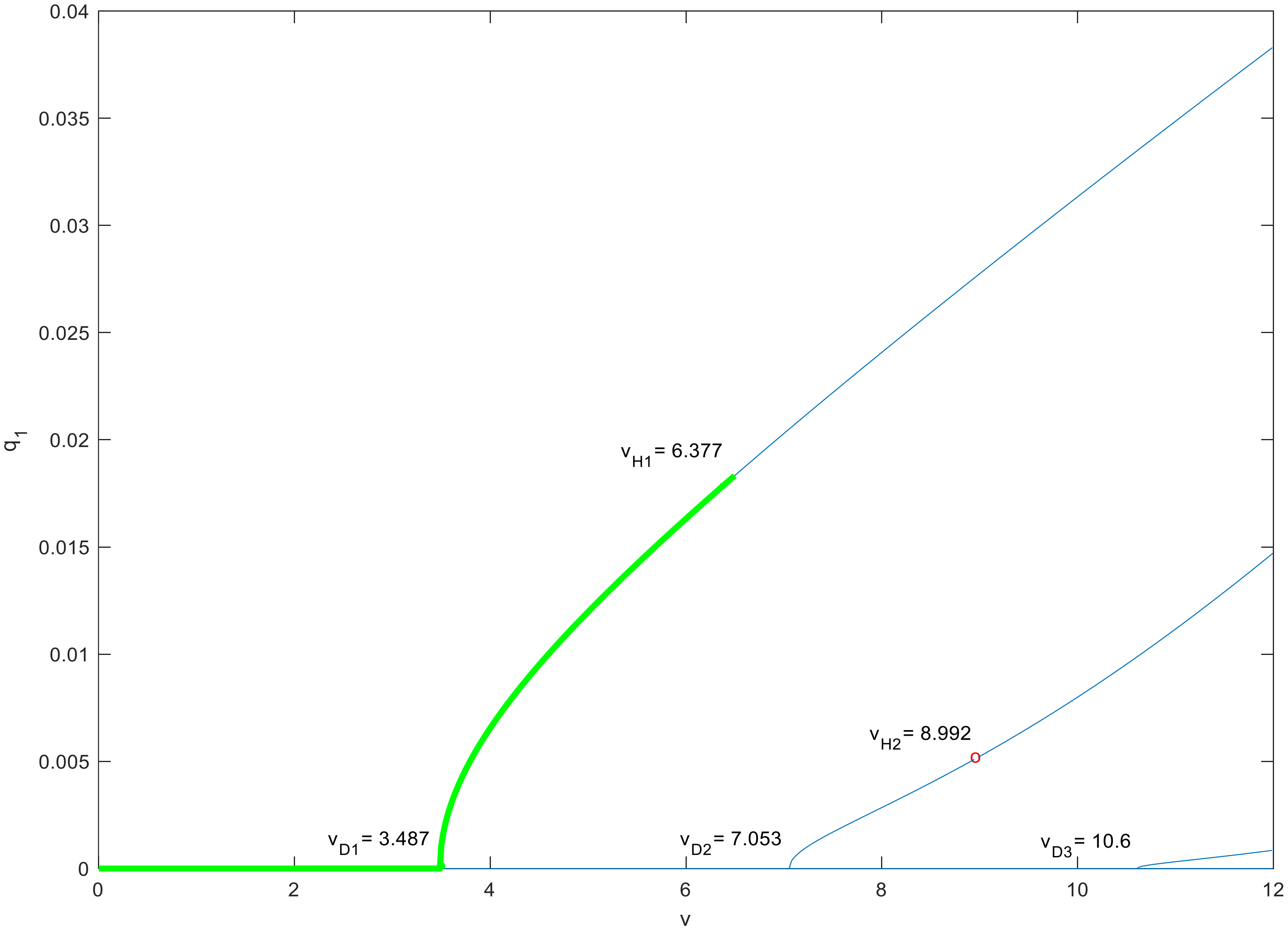

0.04
0.035
0.03
0.025
0.02
0.015
0.01
0.005
0
q_1
0
2
4
6
8
10
12
v
v_{H1}= 6.377
v_{H2}= 8.992
v_{D1}= 3.487
v_{D2}= 7.053
v_{D3}= 10.6

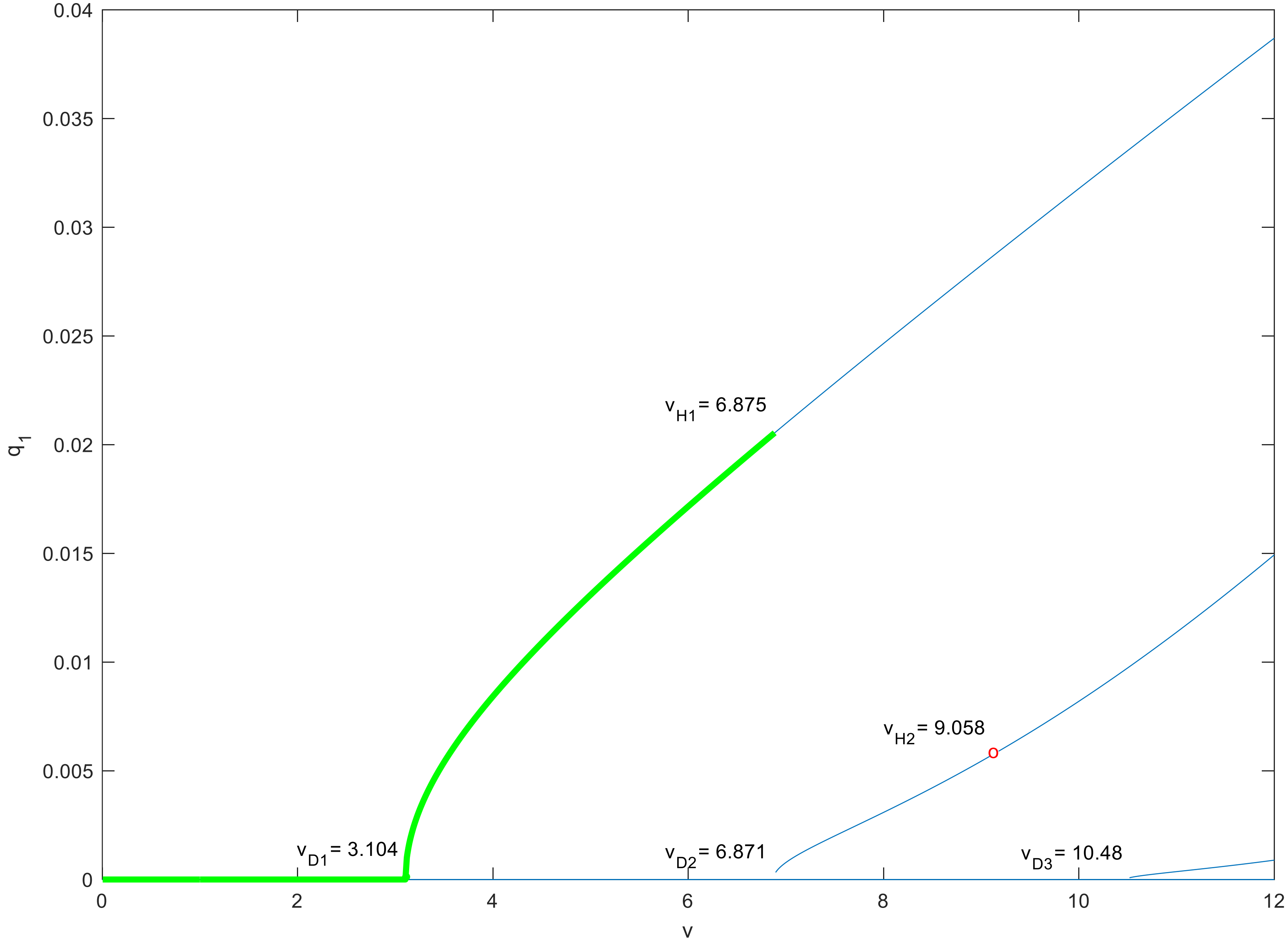
0.04
0.035
0.03
0.025
0.02
0.015
0.01
0.005
0
q_1
0
2
4
6
8
10
12
v
v_{H1}= 6.875
v_{H2}= 9.058
v_{D1}= 3.104
v_{D2}= 6.871
v_{D3}= 10.48

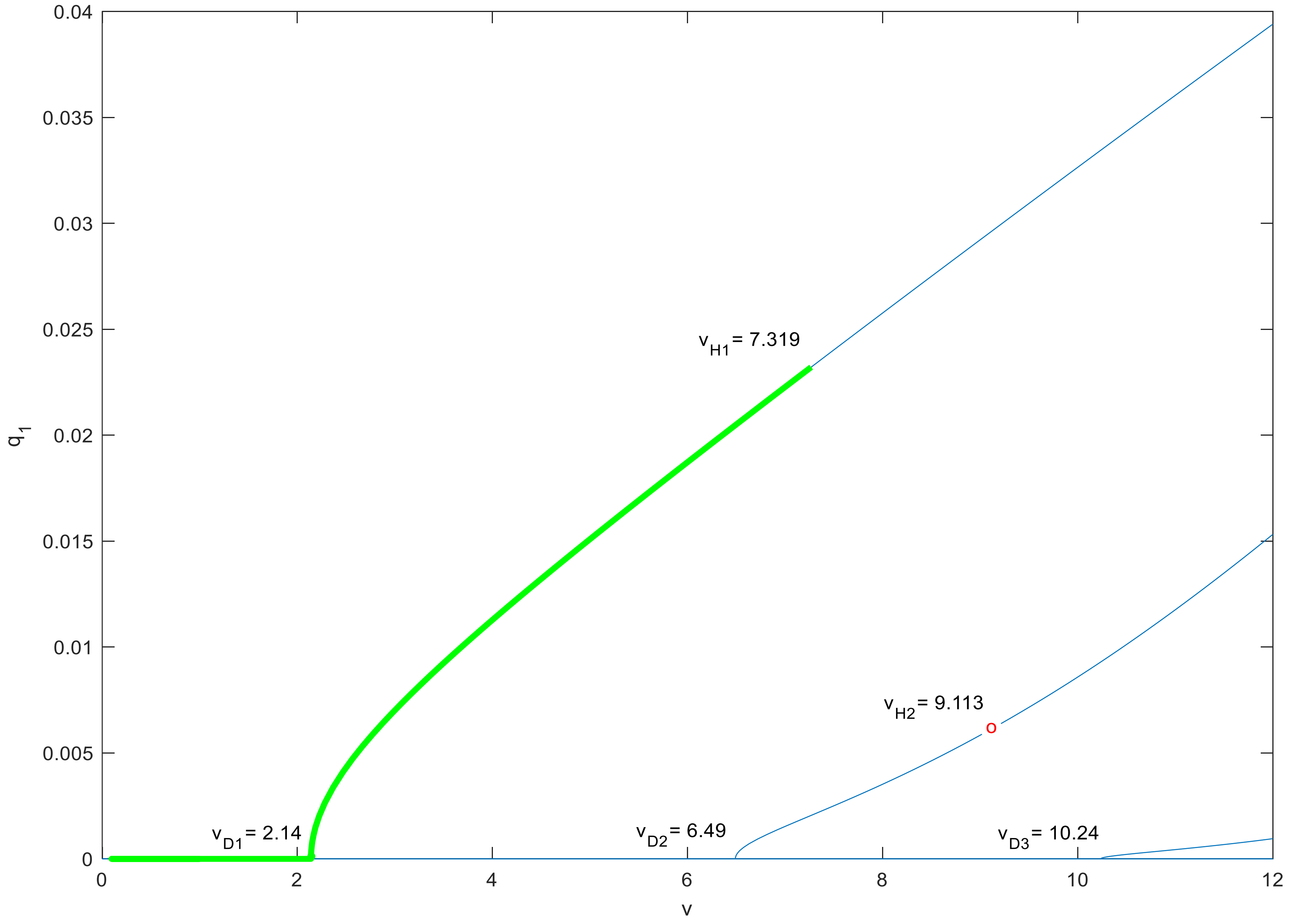

0.04
0.035
0.03
0.025
0.02
0.015
0.01
0.005
0
q_1
0
2
4
6
8
10
12
v
v_{H1}= 7.319
v_{H2}= 9.113
v_{D1}= 2.14
v_{D2}= 6.49
v_{D3}= 10.24

General Trends:

The results obtained through continuation analysis provide the foundationfor the subsequent nonlinear dynamic analysis, where the complex post-criticalbehaviors, including limit cycles, quasi-periodic motions, and chaotic dynamics, are investigated in detail

- In general, increasing internal flow energy causes the system to destabilize via divergence at lower moving speeds, but it delays the dynamic flutter boundary.

NONLINEAR ANALYSIS

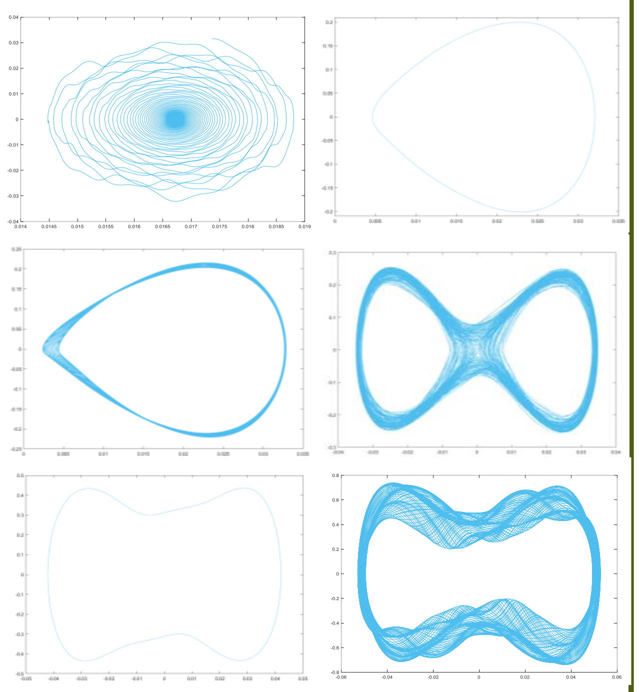

(a) $v = 5$ (b) $v = 6.01$, (c) $v = 6.1$, (d) $v = 6.25$, (e) $v = 6.5$, and (f) $v = 8$

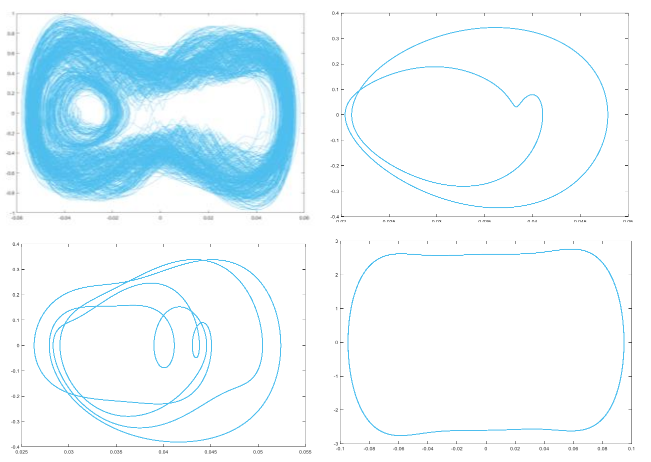

(g) $v = 8.4$, (h) $v = 8.65$, (i) $v = 9.5$, (j) $v = 9.7$

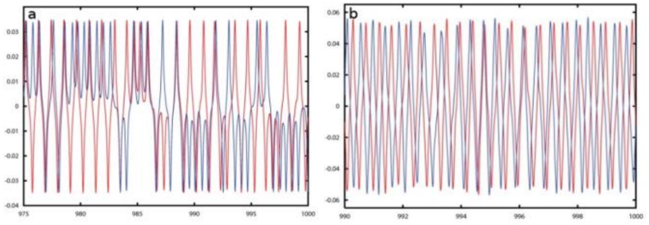

$(a) v = 6.25$ and (b) $v = 8.4$

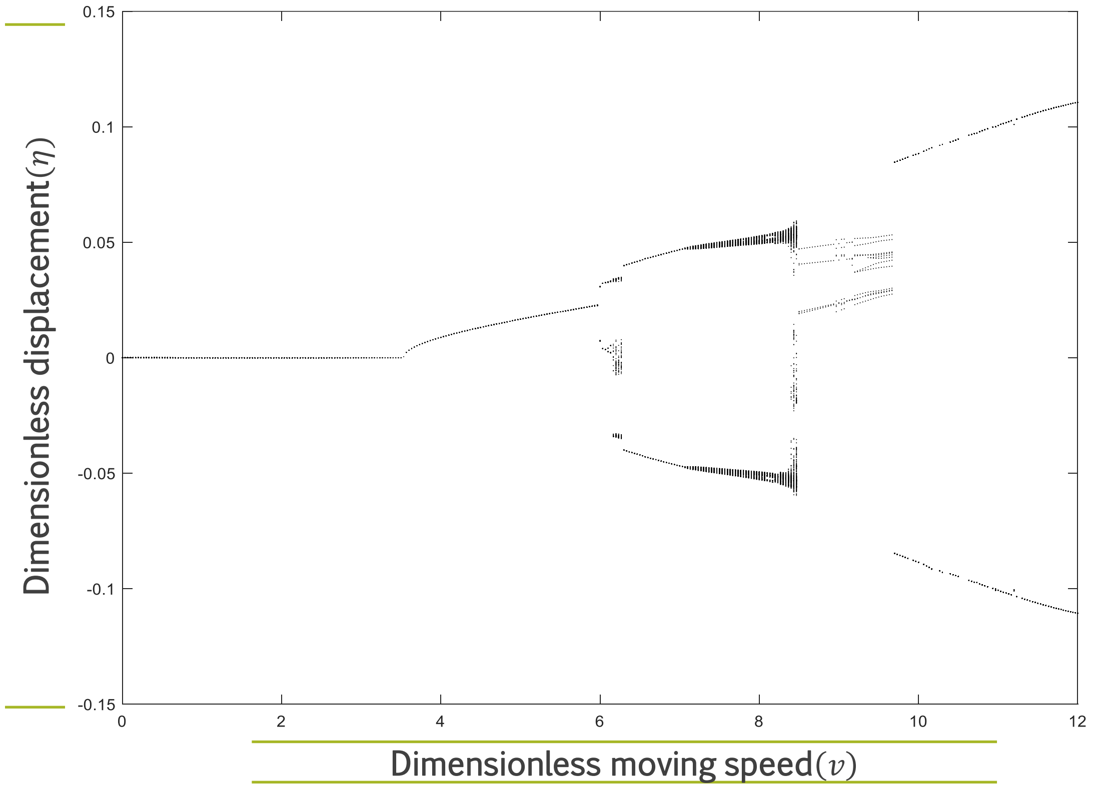

U=0.01

	Divergence	Asymmetric Flutter	Symmetric Flutter	2nd Asymmetric Flutter	Symmetric Flutter
V	3.5	6	6.15	8.65	10.1

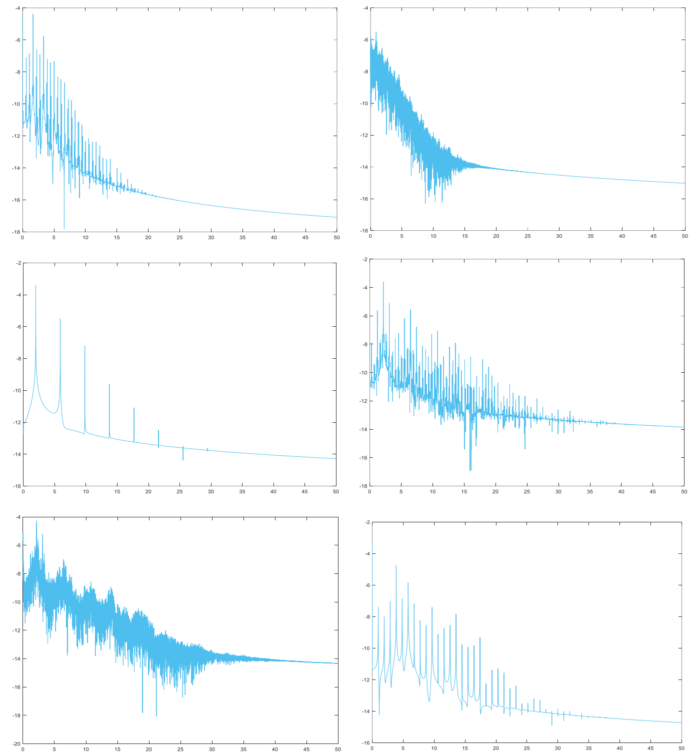

(a) $v = 6.1$, (b) $v = 6.25$, (c) $v = 6.5$, (d) $v = 8$, (e) $v = 8.4$, and (f) $v = 9.5$

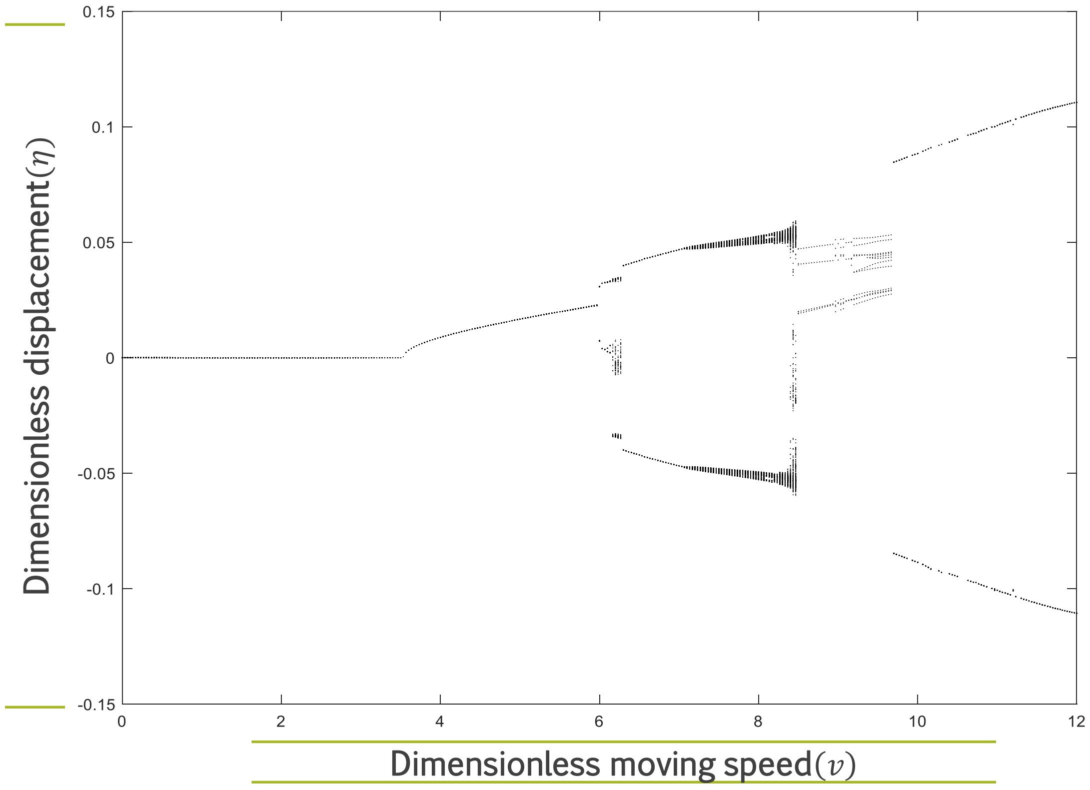

U=0.01

	Divergence	Asymmetric Flutter	Symmetric Flutter	2nd Asymmetric Flutter	Symmetric Flutter
V	3.5	6	6.15	8.65	10.1

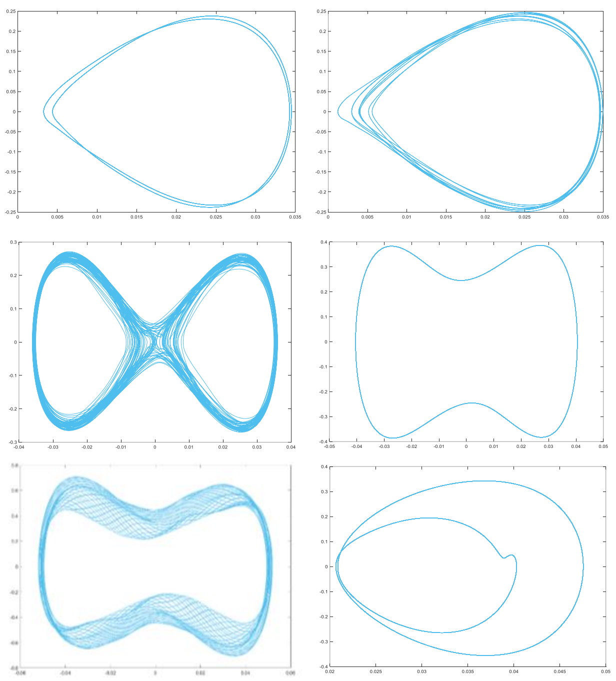

(a) v = 6.25 and (b) v = 6.3, (c) v = 6.4, (d) v = 6.48, (e) v = 8, (f) v = 8.5

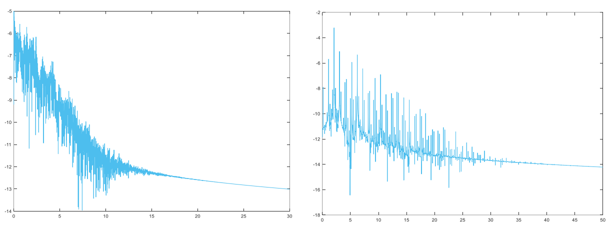

(a) v = 6.4 and (b) v = 8

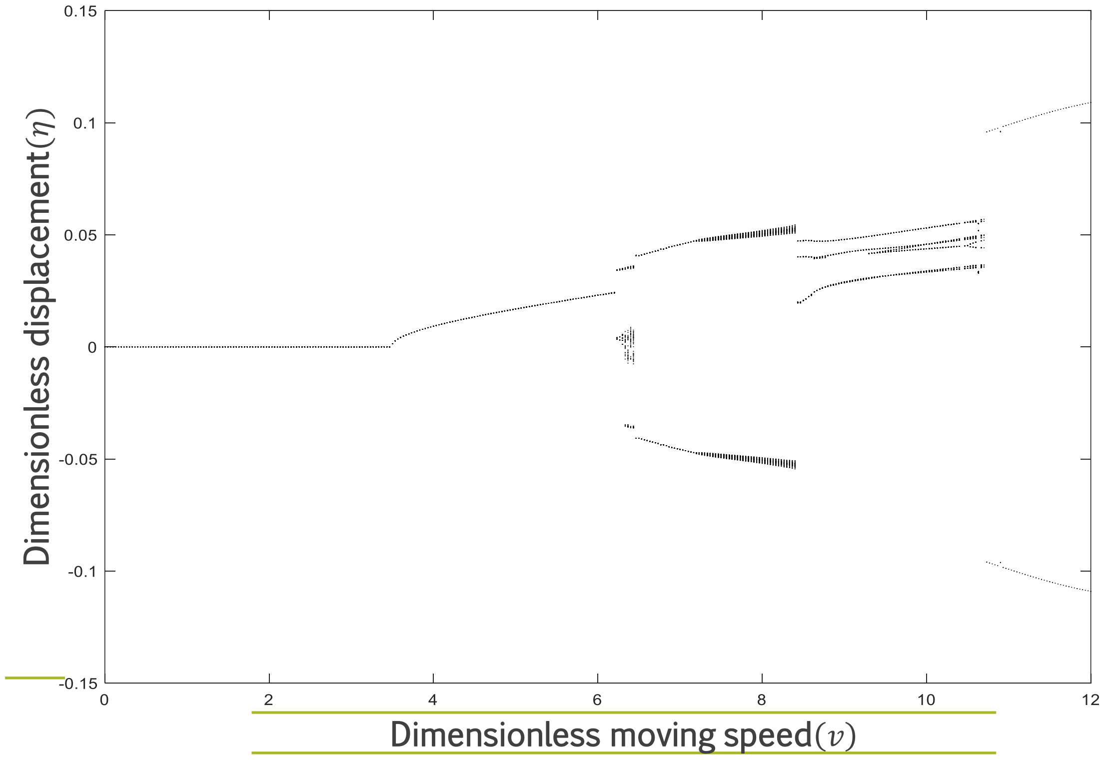

U=0.5

	Divergence	Asymmetric Flutter	Symmetric Flutter	2nd Asymmetric Flutter	Symmetric Flutter
V	3.45	6.25	6.48	8.5	10.8

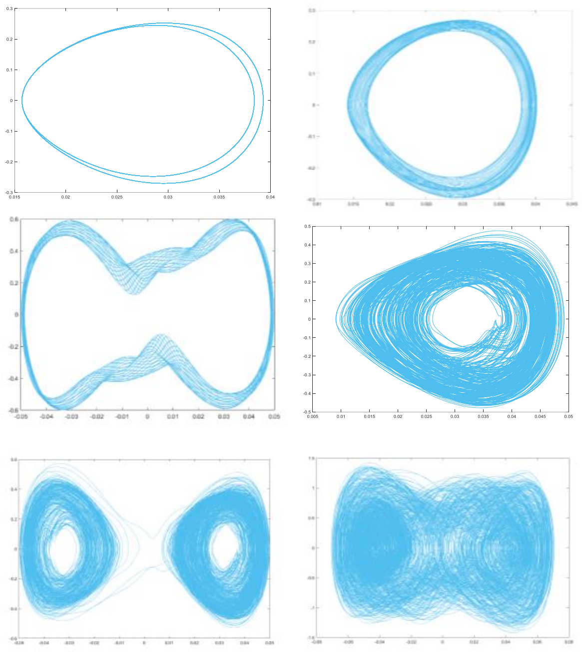

(a) v = 7.1, (b) v = 7.15, (c) v = 7.7, (d) v = 8.1, (e) v = 8.2, and (f) v = 10

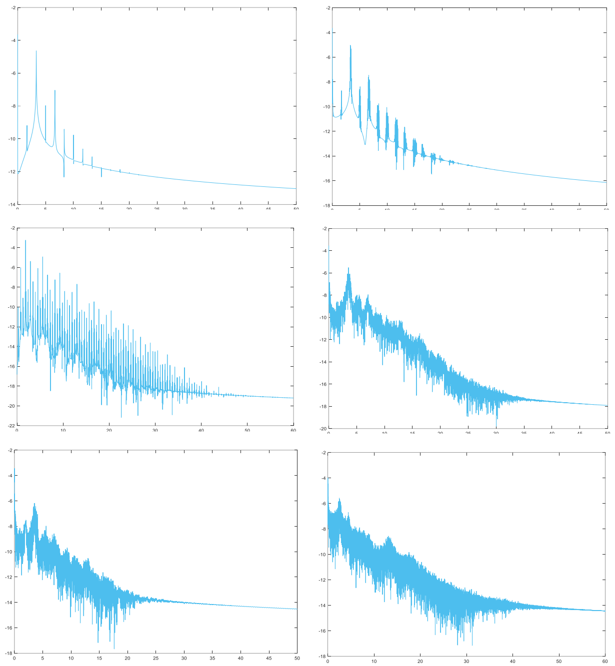

(a) v = 7.1, (b) v = 7.15, (c) v = 7.7, (d) v = 8.1, (e) v = 8.2, and (f) v = 10

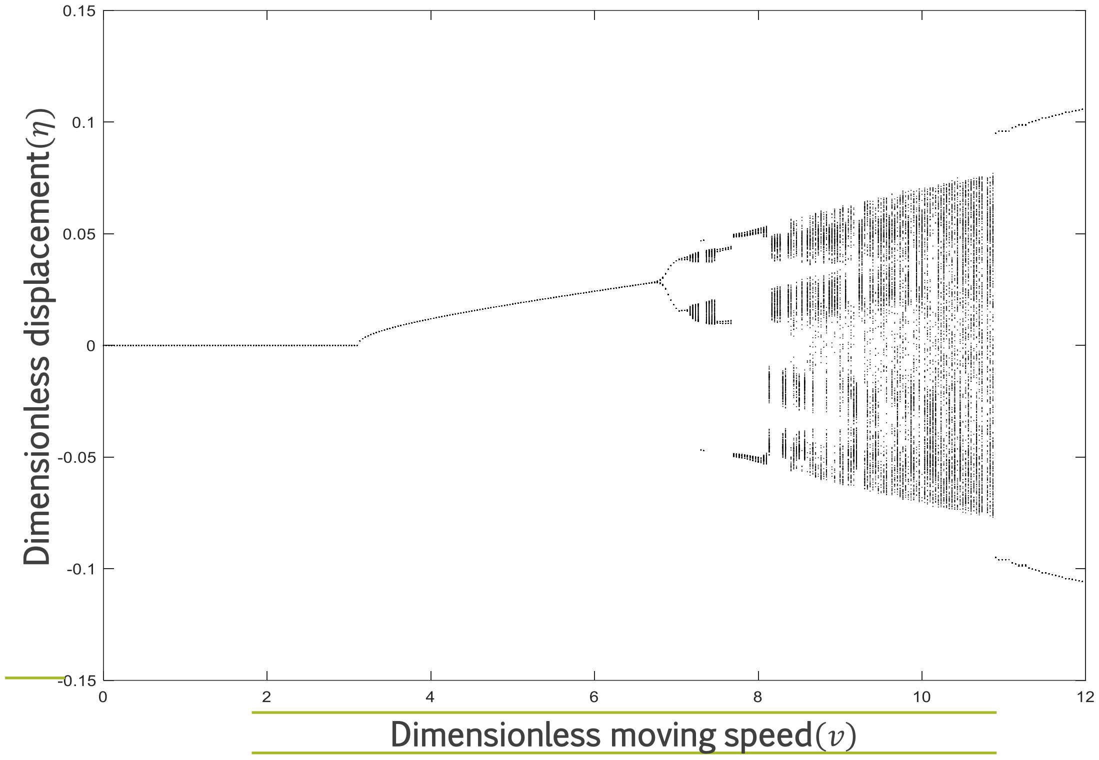

U=1.5

	Divergence	Asymmetric Flutter	Symmetric Flutter	2nd Asymmetric Flutter	Symmetric Flutter
V	3.17	7.1	7.3	8.1	10.2

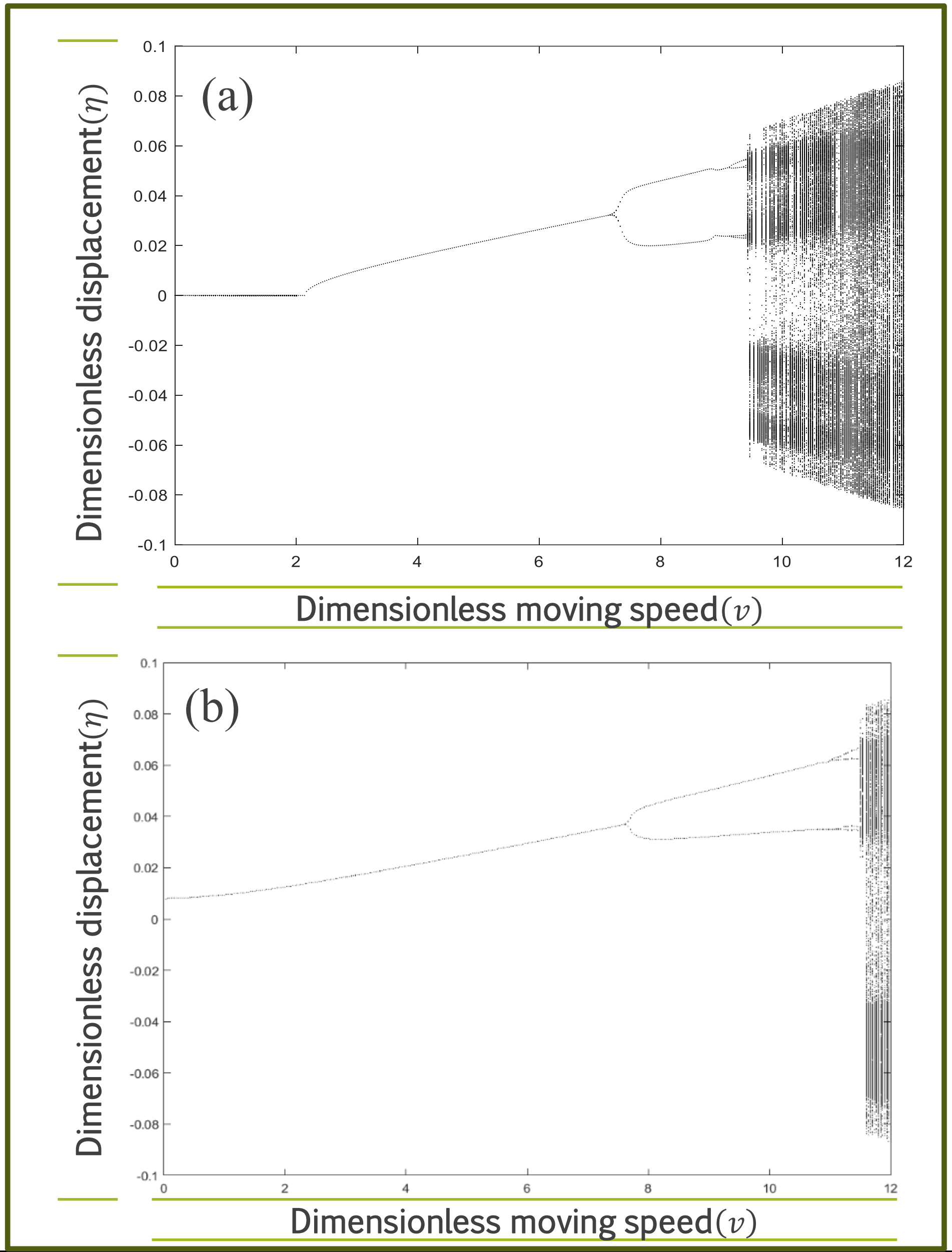

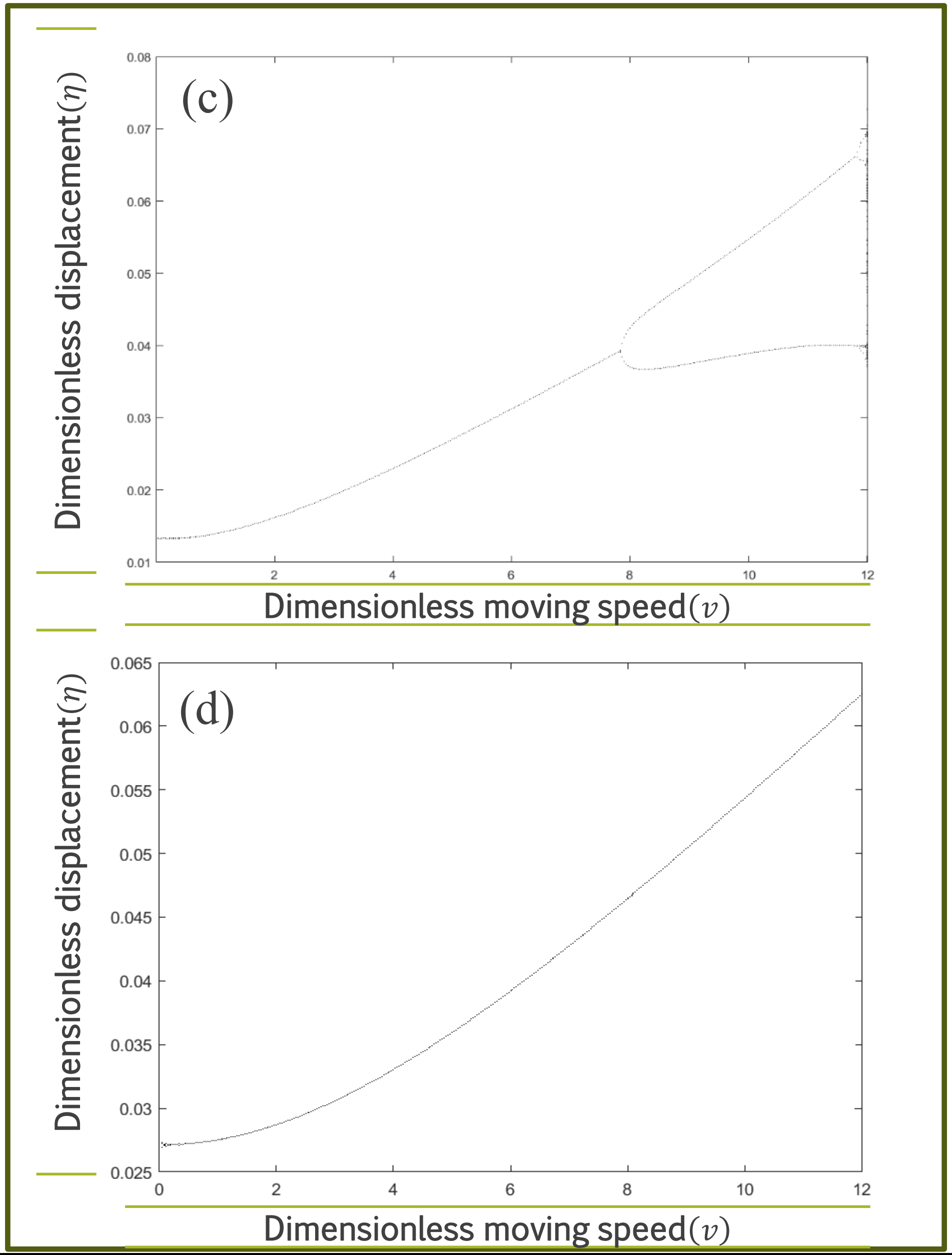

(a) $u = 2.5$
(b) $u = 3.5$
(c) $u = 4$
(d) $u = 6$

General Trends:

- Two fundamental classes of post-critical motion emerge consistently: small-amplitude asymmetric oscillations around post-buckling equilibrium positions and large-amplitude symmetric oscillations around the original static equilibrium, with transitions governed by both moving speed and internal flow velocity.
- A characteristic progression occurs with increasing moving speed: static buckling → asymmetric limit cycles → quasi-periodic motion → chaotic behavior → symmetric limit cycles, demonstrating period-doubling and chaos-to-order transitions typical of nonlinear dynamical systems.
- Higher internal flow velocities ($u > 2.5$) fundamentally alter system behavior by suppressing flutter motion and reducing dynamic complexity. This occurs because internal flow momentum transport dominates support motion effects, causing the system to behave more like a stationary pipe configuration.
- Chaotic motion exhibits sensitive dependence on initial conditions and can manifest in both asymmetric and symmetric forms.
- The existence and extent of chaotic regimes depend on the balance between internal flow energy and support motion parameters.

Thank you for your attention